

# DYNAMIC TRANSITION THEORY FOR THERMOHALINE CIRCULATION

TIAN MA AND SHOUHONG WANG

ABSTRACT. The main objective of this and its accompanying articles is to derive a mathematical theory associated with the thermohaline circulations (THC). This article provides a general transition and stability theory for the Boussinesq system, governing the motion and states of the large-scale ocean circulation. First, it is shown that the first transition is either to multiple steady states or to oscillations (periodic solutions), determined by the sign of a nondimensional parameter  $K$ , depending on the geometry of the physical domain and the thermal and saline Rayleigh numbers. Second, for both the multiple equilibria and periodic solutions transitions, both Type-I (continuous) and Type-II (jump) transitions can occur, and precise criteria are derived in terms of two computable nondimensional parameters  $b_1$  and  $b_2$ . Associated with Type-II transitions are the hysteresis phenomena, and the physical reality is represented by either metastable states or by a local attractor away from the basic solution, showing more complex dynamical behavior. Third, a convection scale law is introduced, leading to an introduction of proper friction terms in the model in order to derive the correct circulation length scale. In particular, the dynamic transitions of the model with the derived friction terms suggest that the THC favors the continuous transitions to stable multiple equilibria. Applications of the theoretical analysis and results to different flow regimes will be explored in the accompanying articles.

## 1. INTRODUCTION

One of the primary goals in climate dynamics is to document, through careful theoretical and numerical studies, the presence of climate low frequency variability, to verify the robustness of this variability's characteristics to changes in model parameters, and to help explain its physical mechanisms. The thorough understanding of this variability is a challenging problem with important practical implications for geophysical efforts to quantify predictability, analyze error growth in dynamical models, and develop efficient forecast methods.

Oceanic circulation is one of key sources of internal climate variability. One important source of such variability is the thermohaline circulation (THC). Physically speaking, the buoyancy fluxes at the ocean surface give rise to gradients in temperature and salinity, which produce, in turn, density gradients. These gradients are, overall, sharper in the vertical than in the horizontal and are associated therefore with an overturning or THC.

---

1991 *Mathematics Subject Classification.* 76A25, 82B, 82D, 37L.

*Key words and phrases.* Thermohaline circulation (THC), dynamic transition theory, multiple equilibria, periodic solutions, effects of frictions, convection scale law.

The work was supported in part by the Office of Naval Research and by the National Science Foundation.

The thermohaline circulation is the global density-driven circulation of the oceans, which is so named because it involves both heat, namely "thermo", and salt, namely "haline". The two attributes, temperature and salinity, together determine the density of seawater, and the differences in density between the water masses in the oceans cause the water to flow.

The thermohaline circulation is also called the great ocean conveyor, the ocean conveyor belt, or the global conveyor belt. The great ocean conveyor produces the greatest oceanic current on the planet. It works in a fashion similar to a conveyor belt transporting enormous volume of cold, salty water from the North Atlantic to the North Pacific, and bringing warmer, fresher water in return. Figure 1.1 gives a simplified map of the great ocean conveyor and Figure 1.2 gives a diagram of oceanic currents of thermohaline circulation.

In oceanography, the procedure of the Conveyor is usually described by starting with what happens in the North Atlantic, under and near the polar region where ice. There warm, salty water that has been northward transported from tropical regions is cooled to form frigid water in vast quantities, which results in a bigger density of seawater (unlike fresh water, saline water does not have a density maximum at  $4^{\circ}\text{C}$  but gets denser as it cools all the way to its freezing point of approximately  $-1.8^{\circ}\text{C}$ ). When this seawater freezes, its salt is excluded (see ice contains almost no salt), increasing the salinity of the remaining, unfrozen water. This salinity makes the water denser again. The dense water then sinks into the deep basin of the sea to form the North Atlantic Deep Water (NADW), and it drives today's ocean thermohaline circulation.

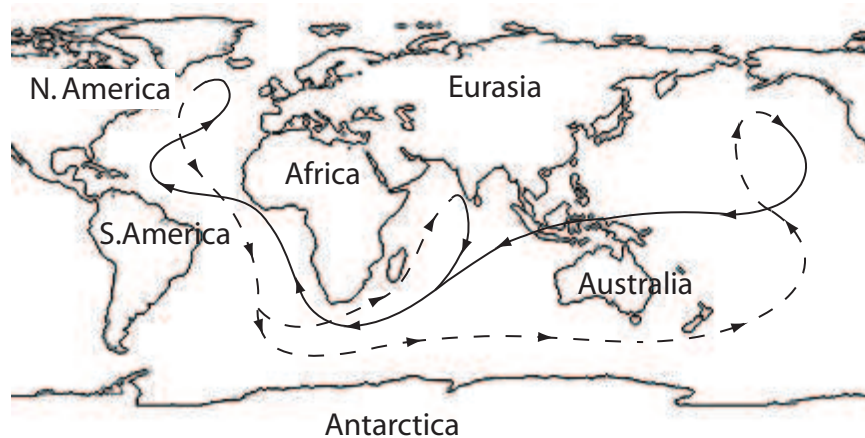


FIGURE 1.1. The diagram of the thermohaline circulation. The dotted line represents deep-water currents, while the solid line represents shallow-water currents.

The sinking, cold and salty water in the North Atlantic flows very slowly and southward into the deep abyssal plains of the Atlantic. The deep water moves then through the South Atlantic around South Africa where it is split into two routes: one into the Indian Ocean and one past Australia into the Pacific. As it continues on its submarine migration, the current mixes with warmer fresh water, and slowly becomes warmer and fresher. Finally, in the North Pacific, the warmer and

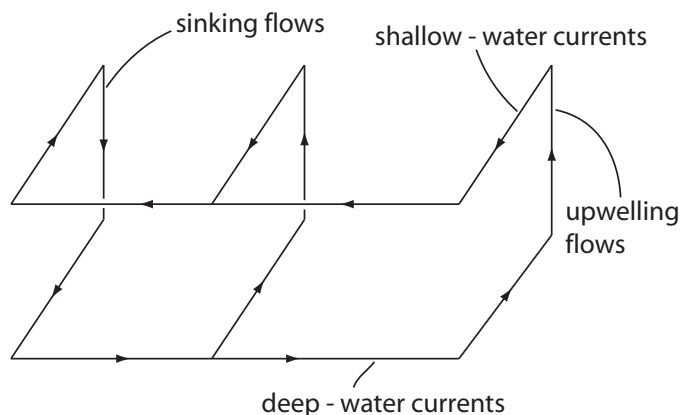


FIGURE 1.2. A schematic diagram of oceanic currents of the global thermohaline circulation.

fresher water upwells, while a shallow-water counter-current has been generated. This counter-current moves southward and westward, through the Indian Ocean, still heading west, and rounding southern Africa, then crosses through the South Atlantic, still on the surface (though it extends a kilometer and a half deep). It then moves up along the east coast of the North America, and on across to the coast of Scandinavia. When this warmer, less salty water reaches high northern latitudes, it chills, and naturally becomes North Atlantic Deep Water, completing its circuit.

The THC varies on timescales of decades or longer, as far as we can tell from instrumental and paleoclimatic data [Martinson et al., 1995]. There have been extensive observational, physical and numerical studies. We refer the interested readers to [3, 2] for an extensive review of the topics; see also among others [33, 29, 11, 9, 27, 28, 34, 35, 36, 4, 5, 6, 7].

The main objective of this series of articles is to study dynamic stability and transitions in large scale ocean circulations associated with THC. A crucial starting point of this theory is that the complete set of transition states are described by a local attractor, rather than some steady states or periodic solutions or other type of orbits as part of this local attractor. Following this philosophy, the dynamic transition theory is recently developed by the authors to identify the transition states and to classify them both dynamically and physically. The theory is motivated by phase transition problems in nonlinear sciences. Namely, the mathematical theory is developed under close links to the physics, and in return the theory is applied to the physical problems, although more applications are yet to be explored. With this theory, many long standing phase transition problems are either solved or become more accessible. In fact, the study of the underlying physical problems leads to a number of physical predictions. For example, the study of phase transitions of both liquid helium-3 and helium-4 [21, 23, 24] leads not only to a theoretical understanding of the phase transitions to superfluidity observed by experiments, but also to such physical predictions as the existence of a new superfluid phase C for liquid helium-3. In return, these physical predictions provides new insights to both theoretical and experimental studies for the underlying physical problems.

The main objective of this article is to provide a theoretical framework for the general Boussinesq equations, which are basic equations describing the motion and states of large scale ocean circulations. Specific applications of the analysis and the results obtained in this article will be explored in the accompanying article in this series, including e.g. the effects of the turbulent frictions and earth's rotation, and circulations in different basins of the ocean. We remark that in collaboration with Hsia, the authors have done preliminary and related work on the dynamic bifurcations of the doubly-diffusive Boussinesq equations [13, 12].

To explain the main results obtained in this paper, we introduce a nondimensional parameter  $K$  defined by:

$$(1.1) \quad K = \text{sign}(1 - \text{Le}) \left[ \frac{\text{Le}^2}{1 - \text{Le}} \left( 1 + \frac{1}{\text{Pr}} \right) \sigma_c - \tilde{R} \right].$$

Here, as defined by (2.7),  $\text{Pr}$  is the Prandtl number,  $\text{Le}$  is the Lewis number,  $R$  is the thermal Rayleigh number, and  $\tilde{R}$  is the saline Rayleigh number. Moreover, the critical number  $\sigma_c$  is defined by (1.2), and can be casted as

$$(1.2) \quad \sigma_c = \min_{\substack{(j,k) \in \mathbb{Z}^2, j,k \geq 0, \\ j^2 + k^2 \neq 0, l \geq 1}} \frac{\pi^4 (j^2 L_1^{-2} + k^2 L_2^{-2} + 1)^3}{j^2 L_1^{-2} + k^2 L_2^{-2}} = \frac{\pi^4 (j_1^2 L_1^{-2} + k_1^2 L_2^{-2} + 1)^3}{j_1^2 L_1^{-2} + k_1^2 L_2^{-2}}.$$

for some integer pair  $(j_1, k_1)$  such that  $j_1 \geq 0$ ,  $k_1 \geq 0$ ,  $j_1^2 + k_1^2 \neq 0$ . Here  $L_1$  and  $L_2$  are the nondimensional length scales in the zonal and meridional directions respectively (with the vertical length scaled to 1).

The analysis in this article shows that the Boussinesq system undergoes a first transition either to multiple equilibria or to periodic solutions (oscillations), dictated by the sign of the nondimensional parameter  $K$ . In the case where  $K > 0$ , the first dynamic transition of the system occurs as the R-Rayleigh number

$$\sigma = R - \text{Le}^{-1} \tilde{R}$$

crosses the critical number  $\sigma$ , leading to multiple equilibria. The transition can either be a Type-I (continuous) transition, or a Type-II (jump) transition, depending on the sign of the following parameter:

$$(1.3) \quad b_1 = \sigma_c - \frac{1 - \text{Le}^2}{\text{Le}^3} \tilde{R}.$$

The Type-II transition leads also to the existence of metastable states, saddle-node bifurcations and the hysteresis associated with it. In this case, as the R-Rayleigh number goes beyond the critical value  $\sigma_c$ , the physical reality is represented by local attractors away from the basic equilibrium state.

In the case where  $K < 0$ , the first transition of the Boussinesq system occurs as the critical C-Rayleigh number

$$\eta = R - \frac{\text{Pr} + \text{Le}}{\text{Pr} + 1} \tilde{R}$$

crosses its first critical value

$$\eta_c = \frac{(\text{Pr} + \text{Le})(1 + \text{Le})}{\text{Pr}} \sigma_c,$$

leading to periodic solutions (oscillatory mode). The spatiotemporal patterns depicted by the oscillatory mode plays an important role in the study of climate

variabilities. As in the previous case, the transition can either be Type-I or Type-II, determined by the sign of another nondimensional parameter  $b_2$  defined by (4.2). As before, in the Type-II transition case, the physical transition states are more complex.

The second part of this article addresses the discrepancies associated with the circulation scales. It is easy to observe that for large scale atmospheric and oceanic circulations, the critical convection scales are often too small. The effects of friction terms to the dynamics in geophysical flows have been studied by many authors; see among many others [26, 2, 10, 30, 31].

The main objective of this part of the study is to propose a turbulent friction term in the Boussinesq equations, leading to correct convection scales. In particular, a basic convective scale law is derived in (5.20). With this scaling law, we are able to propose the correct friction terms in the Boussinesq equations to study THC. With this model, we show that the oceanic THC favors the continuous transition to stable multiple equilibria, rather than other types of transitions.

This article is organized as follows. Section 2 introduces the classical Boussinesq equations and their nondimensional form. Linear analysis is given in Section 3, nonlinear dynamic transitions are studied in Section 4, concluding remarks are given in Section 5. The proof of the main theorems is provided in the appendix.

## 2. BOUSSINESQ EQUATIONS

As mentioned in the Introduction, to demonstrate the basic issues, we ignore the rotational effect of the earth, which will be studied in a forthcoming article. In addition, for simplicity, we regard the region of the Pacific, the Indian Ocean, and the Atlantic, where the ocean conveyor belt occupies, as a rectangular domain:  $\Omega = (0, l_1) \times (0, l_2) \times (0, h)$ , where  $l_1$  stands for the length of this conveyor belt,  $l_2$  for the width, and  $h$  for the deep of the ocean. The motion and states of the large scale ocean are governed by the following Boussinesq equations (see among others [26, 10, 32, 25, 14]):

$$(2.1) \quad \begin{aligned} \frac{\partial u}{\partial t} + (u \cdot \nabla)u &= \nu \Delta u - \frac{1}{\rho_0}(\nabla p + \rho g \vec{k}) \\ \frac{\partial T}{\partial t} + (u \cdot \nabla)T &= \kappa_T \Delta T, \\ \frac{\partial S}{\partial t} + (u \cdot \nabla)S &= \kappa_S \Delta S, \\ \operatorname{div} u &= 0, \end{aligned}$$

where  $u = (u_1, u_2, u_3)$  is the velocity field,  $T$  is the temperature function,  $S$  is the salinity,  $\vec{k} = (0, 0, 1)$ ,  $\kappa_T > 0$  is the thermal diffusivity,  $\kappa_S > 0$  is the salt diffusivity,  $\rho_0 > 0$  is the fluid density at the lower surface  $x_3 = 0$  for  $(x_1, x_2, x_3) \in \Omega$ , and  $\rho$  is the fluid density given by the equation of state

$$(2.2) \quad \rho = \rho_0[1 - a(T - T_0) + b(S - S_0)].$$

Here  $a$  and  $b$  are assumed to be positive constants. Moreover, the lower boundary ( $x_3 = 0$ ) is maintained at a constant temperature  $T_0$  and a constant salinity  $S_0$ , while the upper boundary ( $x_3 = h$ ) is maintained at a constant temperature  $T_1$  and a constant salinity  $S_1$ . The case where  $T_0 < T_1$  and  $S_0 > S_1$  often leads to

thermal and solute stabilities, while each of the following three cases may give rises of instability:

$$(2.3) \quad T_0 > T_1, \quad S_0 < S_1,$$

$$(2.4) \quad T_0 > T_1, \quad S_0 > S_1,$$

$$(2.5) \quad T_0 < T_1, \quad S_0 < S_1.$$

The conditions (2.3)-(2.6) are satisfied respectively over some different regions of the oceans. In particular, in the high-latitude ocean regions the condition (2.3) or (2.4) is satisfied, and in the tropical ocean regions, the case (2.5) occurs. It is these properties (2.3)-(2.5) that give rise to the global thermohaline circulation, and the theoretic results derived in this section also support the viewpoint.

The trivial steady state solution of (2.1)-(2.2) is given by

$$\begin{aligned} u^0 &= 0, \\ T^0 &= T_0 - (T_0 - T_1)x_3/h, \\ S^0 &= S_0 - (S_0 - S_1)x_3/h, \\ p^0 &= p_0 - g\rho_0[x_3 + \frac{a}{2}(T_0 - T_1)x_3^2/h - \frac{b}{2}(S_0 - S_1)x_3^2/h], \end{aligned}$$

where  $p_0$  is a constant. To make the equations nondimensional, we consider the perturbation of the solution from the trivial steady state

$$\begin{aligned} u'' &= u - u^0, & T'' &= T - T^0, \\ S'' &= S - S^0, & p'' &= p - p^0. \end{aligned}$$

Then we set

$$\begin{aligned} x &= hx', & t &= h^2t'/\kappa_T, \\ u'' &= \kappa_T u'/h, & T'' &= (T_0 - T_1)T', \\ S'' &= |S_0 - S_1|S', & p'' &= \rho_0\nu\kappa_T p'/h^2. \end{aligned}$$

Omitting the primes, the equations (2.1) can be written as

$$(2.6) \quad \begin{aligned} \frac{\partial u}{\partial t} &= \text{Pr} (\Delta u - \nabla p) + \text{Pr} (RT - \text{sign}(S_0 - S_1)\tilde{R}S)\bar{k} - (u \cdot \nabla)u \\ \frac{\partial T}{\partial t} &= \Delta T + u_3 - (u \cdot \nabla)T, \\ \frac{\partial S}{\partial t} &= \text{Le} \Delta S + \text{sign}(S_0 - S_1)u_3 - (u \cdot \nabla)S \\ \text{div} u &= 0, \end{aligned}$$

for  $x = (x_1, x_2, x_3)$  in the nondimensional domain

$$\Omega = (0, L_1) \times (0, L_2) \times (0, 1),$$

where  $L_i = l_i/h$  ( $i = 1, 2$ ), and the nondimensional parameters are given by

$$(2.7) \quad \begin{aligned} R &= \frac{ag(T_0 - T_1)h^3}{\kappa_T \nu} && \text{the thermal Rayleigh number,} \\ \tilde{R} &= \frac{bg(S_0 - S_1)h^3}{\kappa_T \nu} && \text{the saline Rayleigh number,} \\ \text{Pr} &= \frac{\nu}{\kappa_T} && \text{the Prandtl number,} \\ \text{Le} &= \frac{\kappa_S}{\kappa_T} && \text{the Lewis number.} \end{aligned}$$

We consider the free boundary condition:

$$(2.8) \quad \begin{aligned} u_1 &= 0, \quad \frac{\partial u_2}{\partial x_1} = \frac{\partial u_3}{\partial x_1} = \frac{\partial T}{\partial x_1} = \frac{\partial S}{\partial x_1} = 0 && \text{at } x_1 = 0, L_1, \\ u_2 &= 0, \quad \frac{\partial u_1}{\partial x_2} = \frac{\partial u_3}{\partial x_2} = \frac{\partial T}{\partial x_2} = \frac{\partial S}{\partial x_2} = 0 && \text{at } x_2 = 0, L_2, \\ u_3 &= T = S = 0, \quad \frac{\partial u_1}{\partial x_3} = \frac{\partial u_2}{\partial x_3} = 0 && \text{at } x_3 = 0, 1. \end{aligned}$$

The initial value conditions are given by

$$(2.9) \quad (u, T, S) = (\tilde{u}, \tilde{T}, \tilde{S}) \quad \text{at } t = 0.$$

For the problem (2.6)-(2.9), we set the spaces

$$\begin{aligned} H &= \{(u, T, S) \in L^2(\Omega)^5 \mid \text{div}u = 0, u \cdot n|_{\partial\Omega} = 0\}, \\ H_1 &= \{(u, T, S) \in H^2(\Omega)^5 \cap H \mid T = S = 0 \text{ at } x_3 = 0, 1\}. \end{aligned}$$

Let  $L_\lambda = A + B_\lambda : H_1 \rightarrow H$  and  $G : H_1 \rightarrow H$  be defined by

$$\begin{aligned} A\psi &= P(\text{Pr } \Delta u, \Delta T, \text{Le } \Delta S), \\ B_x \psi &= P(\text{Pr } (RT - \tilde{R}S \text{sign}(S_0 - S_1))\vec{k}, u_3, \text{sign}(S_0 - S_1)u_3) \\ G(\psi) &= P((u \cdot \nabla)u, (u \cdot \nabla)T, (u \cdot \nabla)S), \end{aligned}$$

for  $\psi = (u, T, S) \in H_1, \lambda = (R, \tilde{R})$ . Here  $P : L^2(\Omega, \mathbb{R}^5) \rightarrow H$  is the Leray projection. Then the problem (2.6)-(2.9) can be written as

$$(2.10) \quad \begin{aligned} \frac{d\psi}{dt} &= L_\lambda \psi + G(\psi), \\ \psi(0) &= \psi_0, \end{aligned}$$

### 3. LINEAR THEORY

**3.1. Eigen-Analysis.** To understand the dynamic transitions of the problem, we need to study the following eigenvalue problem for the linearized equations of (2.6)-(2.8):

$$(3.1) \quad \begin{aligned} \text{Pr } (\Delta u - \nabla p) + \text{Pr } (RT - \tilde{R}S \text{sign}(S_0 - S_1))\vec{k} &= \beta u, \\ \Delta T + u_3 &= \beta T, \\ \text{Le } \Delta S + \text{sign}(S_0 - S_1)u_3 &= \beta S, \\ \text{div}u &= 0, \end{aligned}$$

supplemented with (2.8).

We proceed with the separation of variables. By the boundary condition (2.8),  $\psi = (u, T, S)$  can be expressed in the following form

$$\begin{aligned}
(3.2) \quad & u_1 = u_{jk}(x_3) \sin j\alpha_1\pi x_1 \cos k\alpha_2\pi x_2, \\
& u_2 = v_{jk}(x_3) \cos j\alpha_1\pi x_1 \sin k\alpha_2\pi x_2, \\
& u_3 = w_{jk}(x_3) \cos j\alpha_1\pi x_1 \cos k\alpha_2\pi x_2, \\
& T = T_{jk}(x_3) \cos j\alpha_1\pi x_1 \cos k\alpha_2\pi x_2, \\
& S = S_{jk}(x_3) \cos j\alpha_1\pi x_1 \cos k\alpha_2\pi x_2, \\
& P = P_{jk}(x_3) \cos j\alpha_1\pi x_1 \cos k\alpha_2\pi x_2,
\end{aligned}$$

for integers  $j$  and  $k$ , where  $\alpha_i = L_i^{-1}$  ( $i = 1, 2$ ). Plugging (3.2) into (3.1), we obtain the following sets of ordinary differential equation systems:

$$\begin{aligned}
(3.3) \quad & \text{Pr } D_{jk}u_{jk} + \text{Pr } j\alpha_1\pi p_{jk} = \beta u_{jk}, \\
& \text{Pr } D_{jk}v_{jk} + \text{Pr } k\alpha_2\pi p_{jk} = \beta v_{jk}, \\
& \text{Pr } D_{jk}w_{jk} - \text{Pr } DP_{jk} + \text{Pr } RT_{jk} - \text{Pr } \tilde{R}\text{sign}(S_0 - S_1)S_{jk} = \beta W_{jk}, \\
& D_{jk}T + w_{jk} = \beta T_{jk}, \\
& \text{Le}D_{jk}S_{jk} + \text{sign}(S_0 - S_1)w_{jk} = \beta S_{jk} \\
& j\alpha_1\pi u_{jk} + k\alpha_2\pi v_{jk} + Dw_{jk} = 0, \\
& Du_{jk} = Dv_{jk} = w_{jk} = T_{jk} = S_{jk} = 0 \quad \text{at } x_3 = 0, 1,
\end{aligned}$$

where

$$D = \frac{d}{dz}, \quad D_{jk} = \frac{d^2}{dz^2} - \alpha_{jk}^2, \quad \alpha_{jk}^2 = \pi^2(j^2\alpha_1^2 + k^2\alpha_2^2).$$

If  $w_{jk} \neq 0$ , equations (3.3) can be reduced to a single equation

$$\begin{aligned}
(3.4) \quad & [(D_{jk} - \beta)(\text{Le } D_{jk} - \beta)(\text{Pr } D_{jk} - \beta)D_{jk} \\
& + \text{Pr } R\alpha_{jk}^2(\text{Le } D_{jk} - \beta) - \text{Pr } \tilde{R}\alpha_{jk}^2(D_{jk} - \beta)]w_{jk} = 0, \\
& w_{jk} = D^2w_{jk} = D^4w_{jk} = D^6w_{jk} = 0 \quad \text{at } x_3 = 0, 1,
\end{aligned}$$

It is clear that the solutions of (3.4) are sine functions

$$(3.5) \quad w_{jk} = \sin l\pi x_3 \quad \text{for } (j, k, l) \in \mathbb{Z}^2 \times \mathbb{N}.$$

Substituting (3.5) into (3.4), we see that the corresponding eigenvalues  $\beta$  of Problem (3.1) satisfy the cubic equation

$$\begin{aligned}
(3.6) \quad & \gamma_{jkl}^2(\gamma_{jkl}^2 + \beta)(\text{Le } \gamma_{jkl}^2 + \beta)(\text{Pr } \gamma_{jkl}^2 + \beta) \\
& - \text{Pr } R\alpha_{jk}^2(\text{Le } \gamma_{jkl}^2 + \beta) + \text{Pr } \tilde{R}\alpha_{jk}^2(\gamma_{jkl}^2 + \beta) = 0 \quad \forall (j, k, l) \in \mathbb{Z}^2 \times \mathbb{N}.
\end{aligned}$$

where  $\gamma_{jkl}^2 = \alpha_{jk}^2 + l^2\pi^2$ .

Moreover, to determine  $u_{jk}(x_3), v_{jk}(x_3), T_{jk}(x_3)$ , and  $S_{jk}(x_3)$ , we derive from (3.3) that

$$(3.7) \quad (\text{Pr } D_{jk} - \beta)u_{jk} = -\frac{j\alpha_1\pi}{\alpha_{jk}^2}(\text{Pr } D_{jk} - \beta)Dw_{jk},$$

$$(3.8) \quad (\text{Pr } D_{jk} - \beta)v_{jk} = -\frac{k\alpha_2\pi}{\alpha_{jk}^2}(\text{Pr } D_{jk} - \beta)Dw_{jk},$$

$$(3.9) \quad (D_{jk} - \beta)T_{jk} = -w_{jk},$$

$$(3.10) \quad (\text{Le } D_{jk} - \beta)S_{jk} = -\text{sign}(S_0 - S_1)w_{jk}$$



With the above calculations, all eigenvalues and eigenvectors (3.1) can be derived and are given in the following three groups:

1. For  $(j, k, l) = (j, k, 0)$ , we have

$$\begin{aligned}\beta_{jk0} &= -\text{Pr } \alpha_{jk}^2 = -\text{Pr } (j^2 \alpha_1^2 + k^2 \alpha_2^2), \\ \psi_{jk0} &= (k \alpha_2 \sin j \alpha_1 \pi x_1 \cos k \alpha_2 \pi x_2, -j \alpha_1 \cos j \alpha_1 \pi x_1 \sin k \alpha_2 \pi x_2, 0, 0, 0)\end{aligned}$$

2. For  $(j, k, l) = (0, 0, l)$  with  $l \neq 0$ , we have

$$\begin{aligned}\beta_{00l}^1 &= -l^2 \pi^2, & \beta_{00l}^2 &= -\text{Le } l^2 \pi^2, \\ \psi_{00l}^1 &= (0, 0, 0, \sin l \pi x_3, 0), & \psi_{00l}^2 &= (0, 0, 0, 0, \sin l \pi x_3).\end{aligned}$$

3. For general  $(j, k, l)$  with  $j^2 + k^2 \neq 0$  and  $l \neq 0$ , the solutions  $\beta$  of (3.6) are eigenvalues of (3.1). Let  $\beta_{jkl}^i$  ( $1 \leq i \leq 3$ ) be three zeros of (3.6), with

$$\text{Re} \beta_{jkl}^1 \geq \text{Re} \beta_{jkl}^2 \geq \text{Re} \beta_{jkl}^3.$$

Then, by (3.2), (3.5), and (3.7)-(3.10), the eigenvector  $\psi_{jkl}^i$  corresponding to  $\beta_{jkl}^i$  can be written as

$$(3.11) \quad \psi_{jkl}^i = \begin{cases} u_{jkl}^i \sin j \alpha_1 \pi x_1 \cos k \alpha_2 \pi x_2 \cos l \pi x_3 \\ v_{jkl}^i \cos j \alpha_1 \pi x_1 \sin k \alpha_2 \pi x_2 \cos l \pi x_3 \\ w_{jkl}^i \cos j \alpha_1 \pi x_1 \cos k \alpha_2 \pi x_2 \sin l \pi x_3 \\ T_{jkl}^i \cos j \alpha_1 \pi x_1 \cos k \alpha_2 \pi x_2 \sin l \pi x_3 \\ S_{jkl}^i \cos j \alpha_1 \pi x_1 \cos k \alpha_2 \pi x_2 \sin l \pi x_3, \end{cases}$$

where

$$\begin{aligned}u_{jkl}^i &= -\frac{j \alpha_1 l \pi^2}{\alpha_{jk}^2} = -\frac{j \alpha_1 l}{j^2 \alpha_1^2 + k^2 \alpha_2^2}, & v_{jkl}^i &= -\frac{k \alpha_2 l \pi^2}{\alpha_{jk}^2} = -\frac{k \alpha_2 l}{j^2 \alpha_1^2 + k^2 \alpha_2^2}, \\ w_{jkl}^i &= 1, \\ T_{jkl}^i &= \frac{1}{\gamma_{jkl}^2 + \beta_{jkl}^2}, & S_{jkl}^i &= \frac{\text{sign}(S_0 - S_1)}{\text{Le } \gamma_{jkl}^2 + \beta_{jkl}^2}.\end{aligned}$$

The adjoint equations of (3.1) are given by

$$(3.12) \quad \begin{aligned}\text{Pr } (\Delta u^* - \nabla p^*) + (T^* + \text{sign}(S_0 - S_1) S^*) \vec{k} &= \bar{\beta} u^*, \\ \Delta T^* + \text{Pr } R u_3^* &= \bar{\beta} T^*, \\ \text{Le } \Delta S^* - \text{Pr } \tilde{R} \text{sign}(S_0 - S_1) u_3^* &= \bar{\beta} T^* \\ \text{div } u^* &= 0.\end{aligned}$$

Thus, the conjugate eigenvector  $\psi_{jkl}^{i*}$  of (3.12) corresponding to  $\beta_{jkl}^i$  are as follows

$$(3.13) \quad \psi_{jkl}^{i*} = \begin{cases} u_{jkl}^{i*} \sin j \alpha_1 \pi x_1 \cos k \alpha_2 \pi x_2 \cos l \pi x_3 \\ v_{jkl}^{i*} \cos j \alpha_1 \pi x_1 \sin k \alpha_2 \pi x_2 \cos l \pi x_3 \\ w_{jkl}^{i*} \cos j \alpha_1 \pi x_1 \sin k \alpha_2 \pi x_2 \sin l \pi x_3 \\ T_{jkl}^{i*} \cos j \alpha_1 \pi x_1 \sin k \alpha_2 \pi x_2 \sin l \pi x_3 \\ S_{jkl}^{i*} \cos j \alpha_1 \pi x_1 \sin k \alpha_2 \pi x_2 \sin l \pi x_3, \end{cases}$$

where

$$\begin{aligned} u_{jkl}^{i*} &= u_{jkl}^i = -\frac{j\alpha_1 l \pi^2}{\alpha_{jk}^2}, & v_{jkl}^{i*} &= v_{jkl}^i = -\frac{k\alpha_2 l \pi^2}{\alpha_{jk}^2}, \\ w_{jkl}^{i*} &= 1, \\ T_{jkl}^{i*} &= \frac{\text{Pr } R}{\gamma_{jkl}^2 + \beta_{jkl}^i}, & S_{jkl}^{i*} &= \frac{-\text{sign}(S_0 - S_1) \text{Pr } \tilde{R}}{\text{Re} \tilde{\gamma}_{jkl}^2 + \beta_{jkl}^i}. \end{aligned}$$

Thus, all eigenvectors of (3.1) consist of  $\psi_{jk0}, \psi_{00l}^1, \psi_{00l}^2$ , and  $\psi_{jkl}^i$  ( $i = 1, 2$ ). All conjugate eigenvectors of (3.12) consist of  $\psi_{jk0}^* = \psi_{jk0}, \psi_{00l}^{1*} = \psi_{00l}^1, \psi_{00l}^{2*} = \psi_{00l}^2$ , and  $\psi_{jkl}^{i*}$  as in (3.13).

**3.2. Principle of exchange of stabilities (PES).** The linear stability and instability are precisely determined by the the critical-crossing of the first eigenvalues of (3.1), which is often called PES. For this purpose, we only need to study the solutions  $\beta$  of (3.6), which is equivalent to the following form

$$(3.14) \quad \beta^3 + (\text{Pr} + \text{Le} + 1)\gamma_{jkl}^2\beta^2 + [(\text{Pr} + \text{Le} + \text{Pr Le})\gamma_{jkl}^4 - \text{Pr} \alpha_{jk}^2 \gamma_{jkl}^{-2}(R - \tilde{R})]\beta + \text{Pr Le} \gamma_{jkl}^6 - \text{Pr} \alpha_{jk}^2 (\text{Le} R - \tilde{R}) = 0.$$

As we shall see, both real and complex eigenvalues can occur. The real eigenvalues often lead to transition to steady state solutions, and the complex eigenvalues gives rise oscillations. As we mentioned in the INtroduction, these solutions are related to low frequency variabilities of the oceanic system.

First, we discuss the critical-crossing of the real eigenvalues. To this end we need to introduce a nondimensional parameter, called the R-Rayleigh number, defined by

$$(3.15) \quad \sigma = R - \text{Le}^{-1} \tilde{R} = \frac{gh^3}{\kappa T \nu} (a(T_0 - T_1) - b \text{Le}^{-1}(S_0 - S_1)).$$

It is clear that  $\beta = 0$  is a zero of (3.14) if and only if

$$\text{Le} \gamma_{jkl}^6 - \alpha_{jk}^2 (\text{Le} R - \tilde{R}) = 0.$$

In this case, we have

$$(3.16) \quad \sigma = \frac{\gamma_{jkl}^6}{\alpha_{jk}^2} \geq \sigma_c,$$

where  $\sigma_c$  is defined by (1.2), and is called the *critical R-Rayleigh number*.

Next, we consider the critical-crossing of the complex eigenvalues. For this case, we introduce another nondimensional parameter, called the C-Rayleigh number, defined by

$$(3.17) \quad \eta = R - \frac{\text{Pr} + \text{Le}}{\text{Pr} + 1} \tilde{R} = \frac{gh^3}{\kappa T \nu} \left[ a(T_0 - T_1) - \frac{(\text{Pr} + \text{Le})b}{\text{Pr} + 1} (S_0 - S_1) \right].$$

Let  $i\rho_0$  ( $\rho_0 \neq 0$ ) be a zero of (3.14). Then have

$$\begin{aligned} \rho_0^2 &= (\text{Pr} + \text{Le} + \text{Pr Le})\gamma_{jkl}^4 - \text{Pr} \alpha_{jk}^2 \gamma_{jkl}^{-2}(R - \tilde{R}), \\ \rho_0^2 &= \frac{\text{Pr Le} \gamma_{jkl}^6 - \text{Pr} \alpha_{jk}^2 (\text{Le} R - \tilde{R})}{\gamma_{jkl}^2 (\text{Pr} + \text{Le} + 1)}. \end{aligned}$$

Therefore, equation (3.14) has a pair of purely imaginary solutions  $\pm i\rho_0$  if and only if the following condition holds true

$$(3.18) \quad (\text{Pr} + \text{Le} + 1)(\text{Pr} + \text{Le} + \text{Pr Le})\gamma_{jkl}^6 - \text{Pr} \alpha_{jk}^2(\text{Pr} + \text{Le} + 1)(R - \tilde{R}) \\ = \text{Pr Le} \gamma_{jkl}^6 - \text{Pr} \alpha_{jk}^2(\text{Le} R - \tilde{R}) > 0.$$

It follows from (3.18) that

$$\eta = R - \frac{\text{Pr} + \text{Le}}{\text{Pr} + 1} \tilde{R} = \frac{(\text{Pr} + \text{Le})(1 + \text{Le})}{\text{Pr}} \frac{\gamma_{jkl}^6}{\alpha_{jk}^2}.$$

Hence we define the critical C-Rayleigh number by

$$(3.19) \quad \eta_c = \min_{(j,k,l) \in I} \frac{(\text{Pr} + \text{Le})(1 + \text{Le})}{\text{Pr}} \frac{\gamma_{jkl}^6}{\alpha_{jk}^2} = \frac{(\text{Pr} + \text{Le})(1 + \text{Le})}{\text{Pr}} \frac{\gamma_{j_1 k_1}^6}{\alpha_{j_1 k_1}^2},$$

for the same integer pair  $(j_1, k_1)$  as in (1.2).

**Definition 3.1.** Let  $(j_1, k_1)$  satisfy (1.2). We call  $\sigma_c$  (resp.  $\eta_c$ ) the first critical Rayleigh number if for all eigenvalues  $\beta$  of (3.1) we have

$$\text{Re}\beta(\sigma_c) \leq 0 \quad (\text{resp. } \text{Re}\beta(\eta_c) \leq 0).$$

The following theorem provides a criterion to determine the first critical Rayleigh number for  $\sigma_c$  and  $\eta_c$ , and the proof is given in the appendix.

**Theorem 3.1.** Let  $\text{Le} \neq 1$ , and  $(j_1, k_1)$  satisfy (1.2), and  $\gamma^2 = \gamma_{j_1 k_1}^2$ ,  $\alpha^2 = \alpha_{j_1 k_1}^2$ . Then we have the following assertions:

- (1) If  $K > 0$  where  $K$  is defined by (1.1), then the number  $\sigma_c$  is the first critical Rayleigh number, and

$$(3.20) \quad \beta_{j_1 k_1}^1 \begin{cases} < 0 & \text{if } \sigma < \sigma_c, \\ = 0 & \text{if } \sigma = \sigma_c, \\ > 0 & \text{if } \sigma > \sigma_c, \end{cases}$$

$$(3.21) \quad \text{Re}\beta_{jkl}^r(\sigma_c) < 0 \quad \text{for all } (j, k, l) \text{ not satisfying (1.2)}.$$

- (2) If  $K < 0$ , then the number  $\eta_c$  is the first critical Rayleigh number, and

$$(3.22) \quad \text{Re}\beta_{j_1 k_1}^1 = \text{Re}\beta_{j_1 k_1}^2 \begin{cases} < 0 & \text{if } \eta < \eta_c, \\ = 0 & \text{if } \eta = \eta_c, \\ > 0 & \text{if } \eta > \eta_c, \end{cases}$$

$$(3.23) \quad \text{Re}\beta_{jkl}^r(\eta_c) < 0 \quad \text{for } (j, k, l) \text{ not satisfying (1.2)}$$

This theorem provides a precise criteria on if the first unstable mode corresponds either to multiple equilibrium modes or to oscillatory modes, corresponding to steady state patterns or to spatiotemporal patterns.

#### 4. NONLINEAR DYNAMIC TRANSITIONS

**4.1. Transitions to multiple equilibria.** By Theorem 3.1, we know that under the conditions  $K > 0$  with  $K$  defined by (1.1), the Boussinesq equations (2.6) with (2.8) will have a transition at  $\sigma = \sigma_c$  from real eigenvalues. In this section, we study the transition from a real simple eigenvalue. We know that generically, the first eigenvalues of (3.1) are simple. Hence we always assume that the first real eigenvalue of (3.1) near  $\sigma = \sigma_c$  is simple. Then we have the following results.

**Theorem 4.1.** *Assume that  $\text{Le} \neq 1$ ,  $K > 0$ , and  $b_1 > 0$ , where  $K$  is defined by (1.1), and  $b_1$  is defined by (1.3). Then the problem (2.6) with (2.8) undergoes a Type-I (continuous) transition at the critical R-Rayleigh number  $\sigma_c$ , and the following assertions hold true:*

- (1) *If the R-Rayleigh number  $\sigma$  crosses  $\sigma_c$ , the problem bifurcates to two steady state solutions  $\psi_i^\sigma = (u_i^\sigma, T_i^\sigma, S_i^\sigma)$ ,  $i = 1, 2$ .*
- (2) *There is an open set  $U \subset H$  with  $\psi = 0 \in U$  such that  $\bar{U} = \bar{U}_1 + \bar{U}_2$ ,  $U_1 \cap U_2 = \emptyset$ ,  $\psi = 0 \in \partial U_1 \cap \partial U_2$ , and  $\psi_i^\sigma \in U_i$  attracts  $U_i$  ( $i = 1, 2$ ).*
- (3)  *$\psi_i^\sigma$  can be expressed as*

$$\psi_i^\sigma = (-1)^i a \sqrt{\beta(\sigma)} \psi_{j_1 k_1}^1 + o(\beta^{1/2}(\sigma)) \quad \text{for } i = 1, 2,$$

*where  $a > 0$  is a constant,  $\beta(\sigma) = \beta_{j_1 k_1}^1(\sigma)$  is the first eigenvalue satisfying (B.2), and  $\psi_{j_1 k_1}^1$  is the first eigenvector given by (3.11).*

- (4) *If  $\psi_0 \in U_i$  ( $i = 1, 2$ ), there exists a  $t_0 > 0$  such that when  $t > t_0$ , the velocity component of  $\psi(t, \psi_0)$  is topologically equivalent to the structure as shown in Figure 6.1, with either the same or the reversed orientation. Here  $\psi(t, \psi_0)$  is the solution of (2.6) with (2.8) with initial data  $\psi_0$ .*

**Theorem 4.2.** *Assume that  $\text{Le} \neq 1$ ,  $K > 0$ , and  $b_1 < 0$ . Then the problem (2.6)-(2.8) undergoes a Type-II (jump) transition at  $\sigma_c$ , and the following assertions hold true:*

- (1) *The transition of this problem at  $\sigma_c$  is a subcritical bifurcation, i.e. there are steady state solutions bifurcated on  $\sigma < \sigma_c$ , which are repellers, and no steady state solutions bifurcated on  $\sigma > \sigma_c$ .*
- (2) *There is a saddle-node bifurcation of steady state solutions from  $(\psi_1^*, \sigma^*)$  and  $(\psi_2^*, \sigma^*)$  with  $\sigma^* < \sigma_c$ , and there are four branches of steady state solutions  $\psi_\sigma^i$  ( $1 \leq i \leq 4$ ) in which  $\psi_\sigma^1$  and  $\psi_\sigma^2$  are bifurcated from  $(\psi_1^*, \sigma^*)$ , and  $\psi_\sigma^3, \psi_\sigma^4$  bifurcated from  $(\psi_2^*, \sigma^*)$  on  $\sigma > \sigma^*$ , such that*

$$\lim_{\sigma \rightarrow \sigma_c} \psi_\sigma^1 = \lim_{\sigma \rightarrow \sigma_c} \psi_\sigma^2 = 0, \quad \psi_{\sigma_c}^3, \psi_{\sigma_c}^4 \neq 0,$$

*and  $\psi_\sigma^3$  and  $\psi_\sigma^4$  are attractors for  $\sigma^* < \sigma < \sigma_c + \varepsilon$  with some  $\varepsilon > 0$ .*

**4.2. Transition to oscillatory spatiotemporal patterns.** If the condition  $K < 0$  holds true, by Theorem 3.1, the problem (2.6)-(2.8) will have a transition to the periodic solutions at the critical Rayleigh number  $\eta_c$  given by (3.19). In this section, we discuss the transition from complex eigenvalues. It is easy to see that as  $L_1/L_2 \gg 1$ ,  $\eta_c$  is given by

$$(4.1) \quad \eta_c = \frac{(\text{Pr} + \text{Le})(1 + \text{Le})}{\text{Pr}} \frac{\gamma_{j_1 01}^6}{\alpha_{j_1 0}},$$

for some  $(j_1, k_1) = (j_1, 0)$  with  $j_1 > 0$ . Here, we always assume the condition (4.1) hold true.

In the following, we introduce a parameter which provides a criterion to determine the transition type:

$$(4.2) \quad \begin{aligned} b_2 = & R_c(R_2 B_1 - I_2 B_2)C_3 + R_c(I_2 B_1 + R_2 B_2)C_4 \\ & + \tilde{R}(R_3 B_1 - I_3 B_2)C_5 + \tilde{R}(I_3 B_1 + R_3 B_2)C_6, \end{aligned}$$

where  $\alpha^2 = \alpha_{j_1 0}^2 = j_1^2 \alpha_1^2 \pi^2$ , and

$$\begin{aligned}
R_2 &= \operatorname{Re} A_2(\beta_{J_2}^1(R_{c_2})) = \frac{\alpha^2 + \pi^2}{(\alpha^2 + \pi^2)^2 + \rho^2}, \\
R_3 &= \operatorname{Re} A_3 = \frac{\operatorname{Le}(\alpha^2 + \pi^2)}{\operatorname{Le}^2(\alpha^2 + \pi^2)^2 + \rho^2}, \\
I_2 &= \operatorname{Im} A_2(\beta_{J_2}^1(R_{c_2})) = \frac{-\rho}{(\alpha^2 + \pi^2)^2 + \rho^2}, \\
I_3 &= \operatorname{Im} A_3 = \frac{-\rho}{\operatorname{Le}^2(\alpha^2 + \pi^2)^2 + \rho^2}, \\
B_1 &= \tilde{R} I_3^2 - R_c I_2^2, \\
B_2 &= \tilde{R} I_3 R_3 - R I_2 R_2, \\
C_3 &= -\frac{3R_2}{2\pi} + \frac{\rho^2 R_2}{2\pi(4\pi^4 + \rho^2)} - \frac{\rho\pi I_2}{4\pi^4 + \rho^2}, \\
C_4 &= \frac{I_2}{2\pi} - \frac{\rho^2 I_2}{2\pi(4\pi^4 + \rho^2)} - \frac{\rho\pi R_2}{4\pi^4 + \rho^2}, \\
C_5 &= \frac{3R_3}{2\pi\operatorname{Le}} - \frac{\rho^2 R_3}{2\pi\operatorname{Le}(4\pi^4\operatorname{Le}^2 + \rho^2)} - \frac{\rho I_3}{4\pi^4\operatorname{Le}^2 + \rho^2}, \\
C_6 &= -\frac{I_3}{2\pi\operatorname{Le}} + \frac{\rho^2 I_3}{2\pi\operatorname{Le}(4\pi^4\operatorname{Le}^2 + \rho^2)} - \frac{\rho R_3}{4\pi^4\operatorname{Le}^2 + \rho^2}, \\
\rho^2 &= \frac{\operatorname{Pr}(1 - \operatorname{Le})\tilde{R}}{\operatorname{Pr} + 1} \frac{\alpha^2}{(\alpha^2 + \pi^2)} - \operatorname{Le}^2(\alpha^2 + \pi^2)^2, \\
R_c &= \frac{(\operatorname{Pr} + \operatorname{Le})(1 + \operatorname{Le})}{\operatorname{Pr}} \frac{(\alpha^2 + \pi^2)^3}{\alpha^2} + \frac{\operatorname{Pr} + \operatorname{Le}}{\operatorname{Pr} + 1} \tilde{R}.
\end{aligned}$$

The following theorem characterizes the transition to periodic solutions and the type of the transition.

**Theorem 4.3.** *Let  $b_2$  be given by (4.2), and  $K < 0$  with  $K$  defined by (1.1). Then for problem (2.6)-(2.8), we have the following assertions:*

- (1) *If  $b_2 < 0$ , then the problem has a Type-I transition at  $\eta = \eta_c$ , and bifurcates to a periodic solution on  $\eta > \eta_c$  which is an attractor, the periodic solution can be expressed as*

$$\begin{aligned}
\psi &= x(t)\operatorname{Re}\psi_{j_1 0 1} + y(t)\operatorname{Im}\psi_{j_1 0 1} + o(|x| + |y|), \\
x(t) &= \left( \frac{2\pi\operatorname{Re}\beta(\eta)|\rho|}{|b_2|} \right)^{1/2} \sin \rho t, \\
y(t) &= \left( \frac{2\pi\operatorname{Re}\beta(\eta)|\rho|}{|b_2|} \right)^{1/2} \cos \rho t,
\end{aligned}$$

where  $\beta(\eta) = \lambda(\eta) + i\rho(\eta)$  is the first eigenvalue with  $\lambda(\eta_c) = \operatorname{Re}\beta(\eta_c) = 0$ ,  $\rho(\eta_c) = \rho$  as given in (4.2).

- (2) *If  $b_2 > 0$ , then the transition at  $\eta = \eta_c$  is of Type-II, and there is a singular separation of periodic solutions at some  $(\Gamma^*, \eta^*)$  for  $\eta^* < \eta_c$ , where  $\Gamma^*$  is a periodic solution. In particular, there is a branch  $\Gamma_\eta$  of periodic solutions separated from  $\Gamma^*$  which are repellers, such that  $\Gamma_\eta \rightarrow 0$  as  $\eta \rightarrow \eta_c$ .*

The following example shows that both cases with  $b_2 < 0$  and  $b_2 > 0$  may appear in different physical regimes.

Let  $\rho^2 \cong 0$ . In this case we have

$$\begin{aligned} \tilde{R} &\cong \frac{(\text{Pr} + 1)\text{Le}^2 \gamma^6}{\text{Pr} (1 - \text{Le}) \alpha^2} \begin{cases} > 0 & \text{for } 1 > \text{Le} , \\ < 0 & \text{for } 1 < \text{Le} , \end{cases} \\ R_c &\cong \frac{\text{Pr} + \text{Le}}{\text{Pr} (1 - \text{Le})} \frac{\gamma^6}{\alpha^2}. \end{aligned}$$

Thus, the number  $b_2$  defined by (4.2) is given by

$$\begin{aligned} b_2 &\cong -\gamma^{-12}(R_c - \text{Le}^{-4}\tilde{R})(R_c - \text{Le}^{-3}\tilde{R}) \\ &= \frac{-1}{\text{Pr} \alpha^2(1 - \text{Le})\text{Le}^3}(\text{Le}(\text{Pr} + \text{Le}) - \text{Pr} - 1)(\text{Le}^2(\text{Pr} + \text{Le}) - \text{Pr} - 1). \end{aligned}$$

It is clear that

$$b_2 \begin{cases} < 0 & \text{if } \text{Le} < 1, \\ > 0 & \text{if } \text{Le} > 1. \end{cases}$$

## 5. CONVECTIONS SCALES AND DYNAMIC TRANSITION

**5.1. Convection scale theory.** We investigate a phenomenon appearing in convection problems. For this purpose, we start with the classical Rayleigh-Bénard convection as studied in [16, 19]. In their nondimensional form, the Boussinesq equations are given by

$$\begin{aligned} (5.1) \quad &\frac{1}{\text{Pr}} \left[ \frac{\partial u}{\partial t} + (u \cdot \nabla)u + \nabla p \right] - \Delta u - \sqrt{R}T\vec{k} = 0, \\ &\frac{\partial T}{\partial t} + (u \cdot \nabla)T - \sqrt{R}u_3 - \Delta T = 0, \\ &\text{div} u = 0. \end{aligned}$$

With the free boundary condition:

$$\begin{aligned} (5.2) \quad &u_n = 0, \quad \frac{\partial u_\tau}{\partial n} = 0 \quad \text{on } \partial\Omega, \\ &T = 0 \quad \text{at } x_3 = 0, 1, \\ &\frac{\partial T}{\partial n} = 0 \quad \text{at } x_1 = 0, L_1 \text{ or } x_2 = 0, L_2. \end{aligned}$$

the critical Rayleigh number is

$$(5.3) \quad R_c = \min_{\alpha^2} \frac{(\alpha^2 + \pi^2)^3}{\alpha^2} = \frac{(\alpha_c^2 + \pi^2)^3}{\alpha_c^2} = \frac{27\pi^4}{4},$$

where  $\alpha_c^2 = \frac{\pi^2}{2}$ , and for the Dirichlet (rigid) boundary condition, by Chandrasekha [1],  $R_c$  is

$$(5.4) \quad R_c = 1700.$$

By (5.3) and (5.4), as the horizontal scale  $L$  of the fluid is much larger than its height  $h$ , i.e.  $L \gg h$ , the thermal convection appears at the temperature difference

$$(5.5) \quad T_0 - T_1 = \begin{cases} \frac{27\kappa\nu\pi^4}{4gah^3} & \text{for the free boundary condition,} \\ \frac{1700\kappa\nu}{gah^3} & \text{for the Dirichlet boundary condition.} \end{cases}$$

From (5.5) we see that the critical temperature difference satisfies

$$(5.6) \quad \Delta T_c = T_0 - T_1 \rightarrow \infty \quad \text{if } h \rightarrow 0,$$

$$(5.7) \quad \Delta T_c = T_0 - T_1 \rightarrow 0 \quad \text{if } h \rightarrow \infty.$$

Physically, (5.6) amounts to saying that for a given fluid there is a minimal size  $h_0 > 0$  such that when  $h < h_0$ , no convection occurs for any  $\Delta T = T_0 - T_1 > 0$ . This is in agreement with the fact that in the real world, when  $h$  is small, it is hard to maintain a high temperature gradient to generate the vertical convection.

However, (5.7) has certain physical discrepancies with the energy conservation of the system. In fact, as  $h$  increases, it needs more energy to overcome the friction force to drive fluid to move. With  $\Delta T$  representing this driving force, (5.7) shows that when  $h$  increases,  $\Delta T$  decreases.

Here we present a method to resolve this issue. We note that the critical value  $\alpha^2 = \pi^2/L^2$  stands for the horizontal convection scale  $L$  ( $h$  as its unit):

$$L^2 = \pi^2/\alpha^2.$$

Hence, at the critical value  $\alpha_c^2 = \frac{\pi^2}{2}$  in (5.3), the convective cell size is

$$(5.8) \quad L_c^2 = 2.$$

When  $h$  is not large, this value (5.8) is a good approximation, we need to modify the model to accommodate the case when  $h$  is large.

Instead of (5.8), we propose the convection scale  $L_c$  to be an increasing function of  $h$ :

$$(5.9) \quad L_c^2 = \psi(h), \quad \text{such that } \psi(0) = 2, \psi'(h) > 0.$$

Thus, the critical Rayleigh number  $R_c$  reaches its minimal at

$$(5.10) \quad \alpha_c^2 = \frac{\pi^2}{\psi(h)},$$

rather than at  $\alpha_c^2 = \pi^2/2$ .

The convection scale law of (5.9) and (5.10) should be reflected in the hydrodynamical equations. In other words, we need to revise the Boussinesq equations leading to new critical values given by (5.9) and (5.10). The method we propose here is to include a (turbulent) friction term:

$$(5.11) \quad F = -(\sigma_0 u_1, \sigma_0 u_2, \sigma_1 u_3)$$

in the dimensional form of the Boussinesq equations, where  $\sigma_i$  depends only on  $h$  satisfying

$$(5.12) \quad \sigma_i(0) = 0, \quad \sigma_i'(h) \geq 0, \quad i = 0, 1.$$

Physically, (5.11) and (5.12) stand for the added resistance generated by pressure, also called the damping terms. One can also argue this is due to the averaging to resolve small scale eddies.

In their nondimensional form, the revised Boussinesq equations read

$$(5.13) \quad \begin{aligned} \frac{\partial u}{\partial t} + (u \cdot \nabla)u &= \text{Pr} [\Delta u - \nabla p - f + RT\vec{k}], \\ \frac{\partial T}{\partial t} + (u \cdot \nabla)T &= \Delta T + u_3, \\ \text{div } u &= 0, \end{aligned}$$

where  $f = (\delta_0 u_1, \delta_0 u_2, \delta_1 u_3)$ , and

$$(5.14) \quad \delta_i(h) = \frac{h^2}{\nu} \sigma_i(h), \quad (i = 0, 1).$$

For the revised equations (5.13) with the free boundary conditions (5.2), the critical Rayleigh number is

$$(5.15) \quad R_c = \min_{\alpha^2} \left[ (\alpha^2 + \pi^2) \delta_1 + \frac{(\alpha^2 + \pi^2)^3 + \pi^2(\alpha^2 + \pi^2) \delta_0}{\alpha^2} \right].$$

Let  $g(x) = (x + \pi^2) \delta_1 + ((x + \pi^2)^3 + \pi^2(x + \pi^2) \delta_0)/x$ . Then,  $x_c = \alpha_c^2$  satisfies  $g'(x) = 0$ . Thus we get

$$(5.16) \quad \delta_1 \alpha_c^4 - (\alpha_c^2 + \pi^2)^3 - \pi^2(\alpha_c^2 + \pi^2) \delta_0 + 3\alpha_c^2(\alpha_c^2 + \pi^2)^2 + \pi^2 \alpha_c^2 \delta_0 = 0.$$

We assume that  $\delta_1 > \delta_0$  for  $h \neq 0$ . By  $\alpha_c^2 = \pi^2/L_c^2$ , from (5.11), (5.12) and (5.16) we infer the convection scale law of (5.9) and (5.10). In particular, when  $h$  is large,  $\delta_1 \gg 1$  and  $\delta_1 \gg \delta_0$ , from (5.15) and (5.16) we derive that

$$(5.17) \quad \alpha_c^4 \cong \frac{\pi^4(\pi^2 + \delta_0)}{\delta_1},$$

$$(5.18) \quad L_c^2 \cong \delta_1^{1/2} / (\pi^2 + \delta_0)^{1/2},$$

$$(5.19) \quad R_c \cong \pi^2 \delta_1 + \pi^2 \delta_0 L_c^2,$$

These formulas (5.17)-(5.19) are very useful in studying large-scale convection motion for the height of fluid  $h \geq 10m$ . It can fairly solve the contradiction caused by (5.7). In fact, by (5.14), (5.18) and (5.19) we get the critical temperature difference

$$\Delta T_c = \frac{\pi^2 \kappa \sigma_1(h)}{gah} \quad \text{for } h \gg 1m.$$

It suggests that  $\sigma_1(h) \cong c \cdot h^2$ , leading to the critical temperature gradient being independent of vertical scale  $h$ .

In summary, by (5.14), we propose to take

$$(5.20) \quad \delta_0 = C_0 h^4 / \nu, \quad \delta_1 = C_1 h^4 / \nu,$$

where  $C_0$  and  $C_1$  are constants.

**5.2. Revised Boussinesq equations of the large scale ocean and critical parameters.** Consider the equations (2.1) with a damping term  $\delta u$ . In their nondimensional form, the revised equations of (2.1) are given by

$$(5.21) \quad \begin{aligned} \frac{\partial u}{\partial t} &= \text{Pr} \left[ \Delta u - \delta u + RT \vec{k} - \text{sign}(S_0 - S_1) \tilde{R} S \vec{k} - \nabla p \right] - (u \cdot \nabla) u, \\ \frac{\partial T}{\partial t} &= \Delta T + u_3 - (u \cdot \nabla) T, \\ \frac{\partial S}{\partial t} &= \text{Le} \Delta S + \text{sign}(S_0 - S_1) u_3 - (u \cdot \nabla) S, \\ \text{div} u &= 0, \end{aligned}$$

supplemented with the boundary condition (2.8), where  $\delta u = (\delta_0 u_1, \delta_0 u_2, \delta_1 u_3)$ .



As in (3.6), the eigenvalues of the revised problem satisfy the following equation

$$(5.22) \quad \begin{aligned} & \alpha_{jk}^2 (\gamma_{jk}^2 + \beta) (\text{Le } \gamma_{jk}^2 + \beta) (\text{Pr } \gamma_{jk}^2 + \text{Pr } \delta_1 + \beta) \\ & + \pi^2 (\gamma_{jk}^2 + \beta) (\text{Le } \gamma_{jk}^2 + \beta) (\text{Pr } \gamma_{jk}^2 + \text{Pr } \delta_0 + \beta) \\ & - \text{Pr } R \alpha_{jk}^2 (\text{Le } \gamma_{jk}^2 + \beta) + \text{Pr } \tilde{R} \alpha_{jk}^2 (\gamma_{jk}^2 + \beta) = 0, \end{aligned}$$

which is equivalent to

$$(5.23) \quad \begin{aligned} & \gamma^2 \beta^3 + [\gamma^4 (1 + \text{Pr } + \text{Le } ) + \text{Pr } (\alpha^2 \delta_1 + \pi^2 \delta_0)] \beta^2 \\ & + [(\text{Pr } + \text{Le } + \text{Pr } \text{Le } ) \gamma^6 + \text{Pr } (1 + \text{Le } ) \gamma^2 (\alpha^2 \delta_1 + \pi^2 \delta_0) - \text{Pr } \alpha^2 (R - \tilde{R})] \beta \\ & + \gamma^8 \text{Pr } \text{Le } + \gamma^4 \text{Pr } \text{Le } (\alpha^2 \delta_1 + \pi^2 \delta_0) - \text{Pr } \gamma^2 \alpha^2 (\text{Le } R - \tilde{R}) = 0. \end{aligned}$$

Let  $\beta = 0$ , then we derive from (5.23) the critical Rayleigh number for the first real eigenvalues as

$$(5.24) \quad R_{c_1} = \text{Le}^{-1} \tilde{R} + \min \left[ \gamma^2 \delta_1 + \frac{\gamma^6 + \pi^2 \gamma^2 \delta_0}{\alpha^2} \right],$$

where  $\gamma^2 = \alpha^2 + \pi^2$ . Let  $\beta = i\rho_0$  ( $\rho_0 \neq 0$ ) in (5.23), then we get the critical Rayleigh number for the first complex eigenvalues as follows

$$(5.25) \quad R_{c_2} = \min_{\alpha^2} (\Gamma_1 + \Gamma_2 + \Gamma_3),$$

where

$$\begin{aligned} \Gamma_1 &= \frac{(\text{Pr } + \text{Le } ) \gamma^4 + \text{Pr } (\alpha^2 \delta_1 + \pi^2 \delta_0)}{(\text{Pr } + 1) \gamma^4 + \text{Pr } (\alpha^2 \delta_1 + \pi^2 \delta_0)} \tilde{R}, \\ \Gamma_2 &= \frac{(\text{Pr } + 1) (\text{Pr } + \text{Le } ) (1 + \text{Le } ) \gamma^{10} + \text{Pr } (1 + \text{Le } ) (1 + 2\text{Pr } + \text{Le } ) \gamma^6 (\alpha^2 \delta_1 + \pi^2 \delta_0)}{\text{Pr } \alpha^2 ((\text{Pr } + 1) \gamma^4 + \text{Pr } (\alpha^2 \delta_1 + \pi^2 \delta_0))}, \\ \Gamma_3 &= \frac{\text{Pr}^2 (1 + \text{Le } ) \gamma^2 (\alpha^2 \delta_1 + \pi^2 \delta_0)^2}{\text{Pr } \alpha^2 ((\text{Pr } + 1) \gamma^4 + \text{Pr } (\alpha^2 \delta_1 + \pi^2 \delta_0))}. \end{aligned}$$

It is readily to check that the first eigenvectors of the revised problem are the same as that in (3.11) and (3.13).

For (5.21), we need to modify the transition theorems, Theorems 4.1, 4.2 and 4.3, i.e., to modify the numbers  $b_1$  and  $b_2$  given by (1.3) and (4.2) associated with the new parameters (5.24) and (5.25). Thus, we can make a comparison between the new and old theories.

**5.3. Revised dynamic transition theory.** Linking to the large scale oceanic circulation, we now study the dynamic transition problem for the revised equations (5.21). We start with the introduction of a few typical physical parameters.

**Physical Parameters in Oceanography.** In oceanography, main physical parameters are listed as

$$(5.26) \quad \begin{aligned} \text{Pr} &= 8, & \text{Le} &= 10^{-2}, & a &= 2.1 \times 10^{-4} \text{ K}^{-1}, \\ \nu &= 1.1 \times 10^{-6} \text{ m}^2 \text{ s}^{-1}, & \kappa &= 1.4 \times 10^{-7} \text{ m}^2 \text{ s}^{-1}, & h &= 4 \times 10^3 \text{ m}. \end{aligned}$$

The haline contaction coefficient  $b$  satisfies

$$\begin{aligned} b &= \frac{1}{\rho} \frac{d\rho}{ds} \times 10^{-3}, \\ \rho &= S\rho_S + (1 - S)\rho_W, \end{aligned}$$

where  $S$  is the concentration of salt with unit  $0/_{00}(psu)$ ,  $\rho_S$  and  $\rho_W$  are the densities of salt and water given by

$$\rho_W = 10^3 \text{ kg/m}^3, \quad \rho_S = 1.95 \times 10^3 \text{ kgm}^{-3}.$$

At the sea water density  $\rho = 1.01 \sim 1.05 \times 10^3 \text{ kgm}^{-3}$ , the haline concentration coefficient  $b$  is about

$$b = \frac{1}{\rho}(\rho_S - \rho_W) \times 10^{-3} \cong 0.92 \times 10^{-3}(\text{psu})^{-1}.$$

Thus, for the oceanic motion we obtain the thermal and saline Rayleigh numbers as follows

$$(5.27) \quad R = \frac{ga(T_0 - T_1)}{\kappa\nu} h^3 = 0.86 \times 10^{21}(T_0 - T_1)[^\circ C^{-1}],$$

$$(5.28) \quad \tilde{R} = \frac{gb(S_0 - S_1)}{\kappa\nu} h^3 = 3.75 \times 10^{21}(S_0 - S_1)(\text{psu})^{-1}.$$

For the thermohaline circulation, we know that its scale is tens of thouthands kilometer, namely

$$(5.29) \quad L_c = 0(10^4) \quad (h = 4\text{km as unit}).$$

For the damping coefficients  $\delta_0$  and  $\delta_1$ , by (5.20), we have

$$\delta_i = C_i h^4 / \nu = 2.33 \times 10^{20} C_i \text{ m}^2 \cdot \text{s} \quad (i = 0, 1).$$

Phenomenologically, the constants  $C_i$  depend on the density  $\rho$ , or equivalently on the pressure  $p$ , and we assume that  $C_1$  is proportional to  $\rho$ . Note that the ratio of densities of water and air is about  $10^3$ , i.e.

$$\rho_W / \rho_a \cong 10^3.$$

Therefore, the constant  $C_1$  of water is about  $10^3$  times that of air. Thus, by (5.20), for water we take

$$(5.30) \quad C_1 \approx 10^3(\text{m}^2 \cdot \text{s})^{-1}.$$

However, the constant  $C_0$  depends also on the smoothness of the lower surface. Because the bottom of the sea is more smooth than the lands, this constant  $C_0$  of sea water is not larger than that of air. Thus, we take

$$(5.31) \quad C_0 \cong \frac{1}{2} \times 10^{-12}.$$

Then, we obtain the damping coefficients as

$$(5.32) \quad \delta_0 = 1.17 \times 10^8, \quad \delta_1 = 2.33 \times 10^{23}.$$

We remark that (5.30) and (5.31) are theoretically estimated values. However, they do provide an fairly reasonable explanation to the critical Rayleigh numbers and the convective scales in both the atmospheric and oceanic circulations.

**Critical Rayleigh numbers.** By (5.26) and (5.32),  $\Gamma_1 \simeq \tilde{R}$ , where  $\Gamma_1$  is as defined in (5.25). Thus, the critical Rayleigh numbers (5.24) and (5.25) can be

approximatively expressed as

$$(5.33) \quad R_{c_1} - \text{Le}^{-1} \tilde{R} \cong \min_{\alpha^2} \left[ (\pi^2 + \alpha^2) \delta_1 + \frac{\pi^2 (\pi^2 + \alpha^2) \delta_0}{\alpha^2} \right] \\ \cong \min_{\alpha^2} \left[ (\pi^2 + \alpha^2) \delta_1 + \frac{\pi^4 \delta_0}{\alpha^2} \right],$$

$$(5.34) \quad R_{c_2} - \tilde{R} \cong (1 + \text{Le}) \min_{\alpha^2} \left[ \frac{\text{Pr} + 1}{\text{Pr}} \frac{(\alpha^2 + \pi^2)^5}{\alpha^2 \delta_1 + \pi^2 \delta_0} + \frac{2 \text{Pr} + 1}{\text{Pr}} \frac{(\alpha^2 + \pi^2)^3}{\alpha^2} \right. \\ \left. + (\alpha^2 + \pi^2) \delta_1 + \frac{\pi^2 (\alpha^2 + \pi^2) \delta_0}{\alpha^2} \right] \\ \cong (1 + \text{Le}) \min_{\alpha^2} \left[ (\alpha^2 + \pi^2) \delta_1 + \frac{\pi^4 \delta_0}{\alpha^2} \right].$$

Thus, they have the same  $\alpha_c^2$  given by

$$(5.35) \quad \alpha_c^2 = \pi^2 \left[ \frac{\delta_0}{\delta_1} \right]^{1/2} = 2.24 \times 10^{-7}$$

The convective scale is

$$(5.36) \quad L_c = \frac{\pi}{\alpha_c} = \left[ \frac{\delta_1}{\delta_0} \right]^{1/4} = 0.67 \times 10^4.$$

The critical Rayleigh numbers for real and complex eigenvalues are respectively given by

$$(5.37) \quad \sigma_c = (\pi^2 + \alpha_c^2) \delta_1 + \frac{\pi^4 \delta_0}{\alpha_c^2} = 2.33 \times 10^{23},$$

$$(5.38) \quad \eta_c = (1 + \text{Le}) \sigma_c.$$

Here, as in (3.15) and (3.16), by (5.33) and (5.34), we define the R-Rayleigh number  $\sigma$  and C-Rayleigh number  $\eta$  as follows

$$(5.39) \quad \sigma = R - \text{Le}^{-1} \tilde{R}, \quad \eta = R - \tilde{R}.$$

It is seen that the theoretical value (5.36) agrees with the realistic length scale given in (5.29).

**Revised transition results.** From (5.37)-(5.39) we can see that if

$$\sigma = R - \text{Le}^{-1} \tilde{R} = \sigma_c, \quad \text{and} \quad \eta = R - \tilde{R} < \eta_c = (1 + \text{Le}) \sigma_c,$$

then  $\tilde{R} < \text{Le}^2 \sigma_c / (1 + \text{Le})$ . In this case  $\sigma_c$  is the first critical Rayleigh number.

In addition, if

$$R - \text{Le}^{-1} \tilde{R} = (1 + \text{Le}) \sigma_c, \quad R - \tilde{R} > \sigma_c,$$

then  $\tilde{R} > \text{Le}^2 \sigma_c / (1 + \text{Le})$ , and  $\eta_c$  is the first critical Rayleigh number. Thus, by Theorem 3.1, we obtain the following physical conclusions:

**Physical Conclusion 5.1.** *For the thermohaline circulation, we have the following assertions:*

(1) *If*

$$\tilde{R} < \text{Le}^2 \sigma_c = 2.35 \times 10^{19},$$

*the number  $\sigma_c$  given by (5.37) is the first critical Rayleigh number.*

(2) If

$$\tilde{R} > \frac{\text{Le}^2}{1 - \text{Le}} \sigma_c = 2.35 \times 10^{19},$$

the number  $\eta_c$  given by (5.38) is the first critical Rayleigh number.

Note that the first eigenvectors of the linearized equations of (5.21) are the same as that of (3.1). For the transition of (5.21) from real eigenvalues, the parameter  $b_1$  should be as in (1.3); namely

$$b_1 = \sigma_c - \frac{1 - \text{Le}^2}{\text{Le}^3} \tilde{R}.$$

Here  $R = \sigma_c + \text{Le}^{-1} \tilde{R}$ ,  $\text{Le} = 10^{-2}$ ,  $\sigma_c = 2.33 \times 10^{23}$ ,  $\text{Pr} = 8$ , and  $\alpha_c^2 = 2.24 \times 10^{-7}$ . Thus we have

$$(5.40) \quad b_1 \cong 2.33 \times 10^{17} - \tilde{R},$$

where  $\tilde{R}$  is given by (5.28).

By Theorem 5.3, as  $\tilde{R} < 2.35 \times 10^{19}$  the transition of (5.21) is at  $\sigma = \sigma_c$ . The following theorem is a revised version of Theorems 4.1 and 4.2.

**Physical Conclusion 5.2.** *Let  $\tilde{R} < 2.35 \times 10^{19}$ , and  $b_1$  be as in (5.40). Then the problem (5.21) with (2.8) undergoes a dynamic transition from  $\sigma = \sigma_c$ , and the following assertions hold true:*

- (1) *If  $\tilde{R} < 2.33 \times 10^{17}$ , the transition is continuous, and the problem bifurcates to two steady state solutions  $\psi_1^\sigma$  and  $\psi_2^\sigma$  for  $\sigma > \sigma_c$ ,  $\sigma$  as in (5.39),  $\psi_1^\sigma$  and  $\psi_2^\sigma$  have the expressions as in Assertion (3) of Theorem 4.1, with  $U_1$  and  $U_2$  as their basin of attractions in  $H$  respectively.*
- (2) *If  $2.33 \times 10^{17} < \tilde{R} < 2.35 \times 10^{19}$ , the transition is jump, and there are two saddle-node bifurcations from  $(\psi_1^*, \sigma^*)$  and  $(\psi_2^*, \sigma^*)$  with  $\sigma^* < \sigma_c$ .*
- (3) *When the transition is Type-I, if the initial value  $\tilde{\psi} \in U_i$ , then there is a time  $t_0$  such that as  $t > t_0$ , the velocity component  $u$ , in the solution  $\psi(t, \psi_0)$  with initial value  $\psi_0$ , is topologically equivalent to the structure as shown in Figure 6.1.*

For the transition to periodic solutions, the revised parameters are as follows

$$\begin{aligned} \alpha^2 &= \alpha_c^2 = 2.24 \times 10^{-7} \ll 1, \\ \gamma^2 &= \alpha^2 + \pi^2 \cong \pi^2, \\ R &= R_{c_2} = \tilde{R} + \eta_c \quad (\eta_c \text{ as in (10.208)}). \end{aligned}$$

From (5.23), we can get the imaginary part  $\beta = i\rho$  as

$$\begin{aligned} \rho^2 &= (\text{Pr} + \text{Le} + \text{Pr Le}) \gamma^4 + \text{Pr} (1 + \text{Le}) (\alpha^2 \delta_1 + \pi^2 \delta_0) + \text{Pr} \alpha^2 \eta_c / \gamma^2 \\ &\cong 7.3 \times 10^{16}. \end{aligned}$$

Thus, we derive that

$$\begin{aligned} R_2 &\cong \frac{\pi^2}{\rho^2}, & R_3 &\cong \frac{\text{Le } \pi^2}{\rho^2}, & I_2 &\cong I_3 \cong -\frac{1}{\rho}, \\ C_3 &\cong -\frac{2\pi}{\rho^2}, & C_4 &\cong \frac{\pi(\pi^2 - 2)}{\rho^3}, & C_5 &\cong \frac{\pi + 1}{\rho^2}, \\ C_6 &\cong -\frac{\text{Le } \pi^2(2\pi + 1)}{\rho^3}, & B_1 &\cong \frac{1}{\rho^2}(\tilde{R} - R_{c_2}), & B_2 &\cong \frac{\pi^2(R_{c_2} - \text{Le } \tilde{R})}{\rho^3}. \end{aligned}$$

Then the parameter  $b_2$  in (4.2) reads

$$\begin{aligned} (5.41) \quad b_2 &\cong \frac{\pi}{\rho^6} [\text{Le } \pi(2\pi + 1)\tilde{R}^2 + (\pi^2 - 2)R_{c_2}^2 \\ &\quad - (2\pi^2 - \pi - 2 + \text{Le } \pi(\pi + 2))\tilde{R}R_{c_2}] \\ &\cong \frac{\pi}{\rho^6} [-(1 - \text{Le})\pi(\pi - 1)\tilde{R}^2 + (\pi^2 - 2)\eta_c^2 \\ &\quad + (\pi - 2 - \text{Le } \pi^2 - 2\text{Le } \pi)\tilde{R}\eta_c] \\ &\cong \frac{\pi}{\rho^6} [-\pi(\pi - 1)\tilde{R}^2 + (\pi^2 - 2)\eta_c^2 + \tilde{R}\eta_c]. \end{aligned}$$

Then Theorem 4.3 is rewritten as

**Physical Conclusion 5.3.** *Let  $\tilde{R} > 2.35 \times 10^{19}$ , and  $b_2$  be the parameter as in (5.41). Then for the problem (5.21) with (2.8), Assertions (1) and (2) of Theorem 4.3 hold true.*

## 6. THC DYNAMICS

The above Physical Conclusions 5.1-5.3 provide the possible dynamical behaviors for the great ocean conveyor, depending on the saline Rayleigh number  $\tilde{R}$ .

We note that the temperature and salinity differences  $T_0 - T_1$  and  $S_0 - S_1$  between the oceanic bottom and upper surfaces are different from the observed data. In fact, the observed values should be as follows

$$\begin{aligned} \Delta T &= T_0 - T_1 + T(x_1, x_2, 0) - T(x_1, x_2, 1), \\ \Delta S &= S_0 - S_1 + S(x_1, x_2, 0) - S(x_1, x_2, 1), \end{aligned}$$

where  $T(x)$  and  $S(x)$  are the transition solutions as described by Assertion (3) of Theorem 4.1. Due to the heat resources coming from the earth's crust, the bottom temperature  $T_0$  of the ocean retains essentially a constant, and the bottom salinity  $S_0$  is also a constant which equals to the average value

$$S_0 = \frac{1}{|V|} \int_V S(x) dx, \quad |V| \text{ the volume of the ocean.}$$

It is easy to see that on the upper surface, the temperature and salinity vary in different regions. In the equator,  $T$  is about  $20 \sim 40^\circ C$  and near the Poles,  $T$  is  $2 \sim -1.8^\circ C$ . Here,  $T_1$  takes an average on the upper surface. Since the elevated rate of evaporation in the tropical areas and the freezing of polar sea ice, which leave the salt behind in the remaining seawater, the densities of tropical and polar water are quite high. Hence, as an average, we determine that

$$(6.1) \quad T_0 - T_1 \leq 0, \quad S_0 - S_1 < 0.$$

By Physical Conclusion 5.1 and (6.1), the saline Rayleigh number  $\tilde{R} < 0$ . Therefore the transition of (5.21) with (2.8) is from real eigenvalues. In addition, by  $\tilde{R} < 0$ , we see that the number in (5.40) satisfies that  $b_1 > 0$ . Thus, by Physical Conclusion 5.2, the dynamical behavior of the THC is a Type-I transition to a pair of stable equilibrium states provided

$$\sigma = R - \text{Le}^{-1}\tilde{R} > \sigma_c,$$

which, by (5.27), (5.28) and (5.37), is equivalent to

$$(6.2) \quad 0.86 \times 10^{21}(T_0 - T_1) + 3.75 \times 10^{23}(S_1 - S_0) > 2.33 \times 10^{23}.$$

For the large scale ocean circulation,  $T_0 - T_1 < 100^\circ\text{C}$ . Hence, (6.2) shows that if  $S_1 - S_0 = O(1)$ , then the great ocean conveyor is driven by the doubly-diffusive convection.

In Assertion (1) of Physical Conclusion 5.2, the steady state solutions describing the great Conveyor are approximatively expressed by

$$(6.3) \quad v^\pm = \begin{cases} \pm C\beta^{1/2}(\sigma)L_1 \sin \frac{\pi x_1}{L_1} \cos \pi x_3, \\ \mp C\beta^{1/2}(\sigma) \cos \frac{\pi x_1}{L_1} \sin \pi x_3, \end{cases}$$

$$(6.4) \quad T^\pm = T_0 + (T_1 - T_0)x_3 \mp \frac{C\beta^{1/2}(\sigma)}{\alpha_c^2 + \pi^2} \cos \frac{\pi x_1}{L_1} \sin \pi x_3,$$

$$(6.5) \quad S^\pm = S_0 + (S_1 - S_0)x_3 \mp \frac{\text{sign}(S_0 - S_1)C\beta^{1/2}}{\text{Le}(\alpha_c^2 + \pi^2)} \cos \frac{\pi x_1}{L_1} \sin \pi x_3,$$

where  $C > 0$  is a constant,  $\beta(\sigma)$  is the first real eigenvalue, and by the eigenvalue crossing properties in [22],  $\beta(\sigma)$  can be expressed as

$$(6.6) \quad \beta(\sigma) = k(\sigma - \sigma_c) + o(|\sigma - \sigma_c|)$$

for some constant  $k > 0$ .

In oceanic dynamics, the Rayleigh number  $\sigma = R - \text{Le}^{-1}\tilde{R}$  is a main driving force for the great ocean conveyor, (6.3) and (6.6) show that the velocity  $v$  of the oceanic circulation is proportional to  $\sqrt{\sigma - \sigma_c}$ .

The velocity field  $v^+$  given by (6.3) is topologically equivalent to the structure as shown in Figure 6.1, which is consistent with the real oceanic flow structure.

Assertion (3) in the Physical Conclusion 5.2 shows also that the theoretical results are in agreement with the real thermohaline ocean circulation.

At  $x_3 = 1/2$ , the temperature  $T^+$  and salinity  $S^+$  given by (6.4) and (6.5) are as follows

$$T_{1/2}^+(x_1) = \frac{1}{2}(T_0 + T_1) - \frac{C\beta^{1/2}}{\alpha_c^2 + \pi^2} \cos \frac{\pi x_1}{L_1},$$

$$S_{1/2}^+(x_1) = \frac{1}{2}(S_0 + S_1) + \frac{C\beta^{1/2}}{\text{Le}(\alpha_c^2 + \pi^2)} \cos \frac{\pi x_1}{L_1}.$$

The distributions  $T_{1/2}^+(x_1)$  and  $S_{1/2}^+(x_1)$  are illustrated by Figures 6.2 and 6.3 respectively. In particular, if  $x_1 = 0$  stands for the North Atlantic,  $x_1 = L_1$  for the North Pacific, and  $x_3 = 1/2$  for the deep basin of the ocean, then the profiles of  $T_{1/2}^+(x_1)$  and  $S_{1/2}^+(x_1)$  confirm with observations, in where the North Atlantic Deep Water is cold and salty water, and the North Atlantic Deep Water is warmer and fresher water.

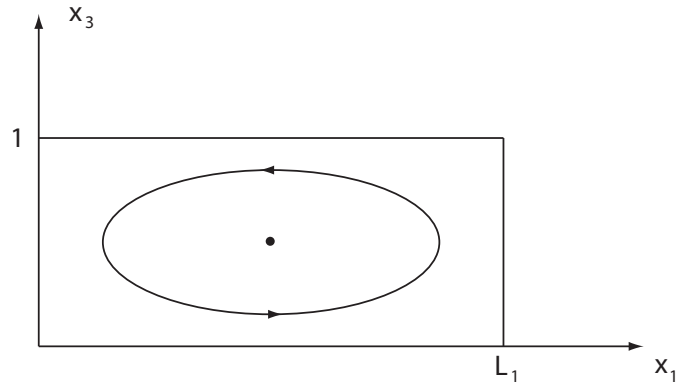


FIGURE 6.1. The flow structure described by  $v^+$  in (6.3).

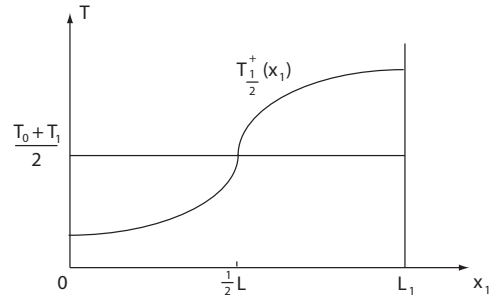


FIGURE 6.2. The temperature profile in deep water of the ocean.

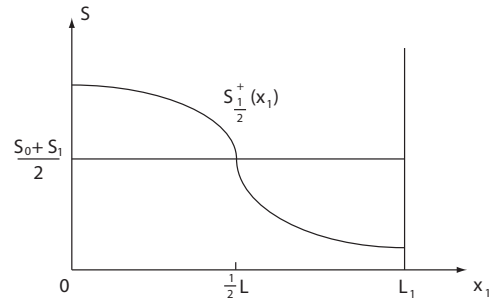


FIGURE 6.3. The salinity profile in deep water of the ocean.

Physical Conclusions 5.1 and 5.2 show that although the THC is mainly due to a continuous transition to multiple equilibria, analysis for other possible dynamical behaviors is still interesting.

We can see that when  $\tilde{R}$  satisfies

$$(6.7) \quad \frac{\text{Le}^3}{1 - \text{Le}^2} \sigma_c < \tilde{R} < \frac{\text{Le}^2}{1 - \text{Le}} \sigma_c,$$

the number  $b_1$  in (5.40) is less than zero, i.e.  $b_1 < 0$ , then due to Physical Conclusions 5.1 and 5.2, the transition is jumping, leading to a saddle-node oscillation.

When  $\tilde{R} > \frac{Le^2}{1-Le} \sigma_c = 2.35 \times 10^{19}$ , the problem undergoes a dynamic transition to a periodic solution, as  $\eta > \eta_c$ . This transition can be either Type-I, or Type-II, described as follows:

First, if  $\tilde{R} > 2.35 \times 10^{23}$ , the number  $b_2$  in (5.41) is less than zero, and by Physical Conclusion 5.3, this system undergoes a Type-I transition to a stable periodic solution as  $\eta = R - \tilde{R} > \eta_c$ , its velocity field is written as

$$(6.8) \quad u(x, t) = \begin{cases} - \left( \frac{2\pi\lambda(\eta)}{|b_2|} \right)^{1/2} L_1 \sin \rho_0 t \sin \frac{\pi x_1}{L_1} \cos \pi x_3, \\ \left( \frac{2\pi\lambda(\eta)}{|b_2|} \right)^{1/2} \sin \rho_0 t \cos \frac{\pi x_1}{L_1} \sin \pi x_3, \end{cases}$$

where  $\lambda(\eta) = \text{Re}\beta_1(\eta)$ ,  $\eta = R - \tilde{R}$ , and  $\rho_0$  is as in (5.41).

Second, if  $2.35 \times 10^{19} < \tilde{R} < 2.35 \times 10^{23}$ , the number  $b_2 > 0$ . Hence the transition is jump to a stable periodic solution at  $\eta = \eta_c$ , leading to an oscillation between a time-periodic solution and the trival equilibrium near  $\eta_c$ .

Finally, some remarks for the oceanic thermohaline circulation are in order.

First, the condition (6.1) provides a more realistic scenario, where  $\tilde{R}$  satisfies that  $\tilde{R} < \frac{Le^3}{1-Le^2} \sigma_c$ . In this case the circulation is a continuous transition to multiple stable equilibria, with flow structure as illustrated by Figure 6.1, and with the temperature and salinity profiles for deep water of the ocean as shown in Figures (6.2)-(6.3). This is consistent with observations.

Second, it is known that the velocity takes  $\kappa/h$  as its unit. Thus, the maximal value of  $v_1$  in (6.3) is that  $v_{\max} = CL_1\kappa h^{-1}\beta^{1/2}$ , where  $C = \left(\frac{Pr}{8}b_1\right)^{-1/2}$ ,  $b_1$  is the number given by (5.40), and  $b_1 \cong \frac{100}{8}$ . From (5.26) and (5.36) we get

$$v_{\max} = \frac{\kappa L_1}{\sqrt{b_1} h} \beta^{1/2}(\sigma) = 0.64 \times 10^{-7} \beta^{1/2}(\sigma) \text{m/s}.$$

The theoretical velocity is very small. In addition, the ratio between the vertical and horizontal velocities is given by

$$\frac{v_3}{v_1} = \frac{1}{L_1} = 1.56 \times 10^{-4}.$$

As a contrast, the oceanic circulation takes about 1600 years for its a journey, i.e., the real velocity is also very small.

Third, the condition (6.7) would lead to a saddle-node bifurcation to metastable states. However, these state have not been observed in oceanography.

Fourth, if  $\tilde{R} > 2.35 \times 10^{23}$ , then the circulation is time-periodic, and we see from (6.8) that the period is

$$\tau = \frac{2\pi}{\rho_0} \cdot \frac{h^2}{\kappa} = 1.1 \times 10^6 \text{s}.$$

where  $\rho_0$  is as in (5.41), and  $\rho_0 \cong 6.5 \times 10^8$ . This period is about four months. It is not realistic.

Fifth, when  $2.35 \times 10^{19} < \tilde{R} < 2.35 \times 10^{23}$ , the oceanic system undergoes a time-periodic oscillation phenomenon. However, this behavior has not been observed in a realistic oceanic regime.



## 7. CONCLUDING REMARKS

Two criteria are derived in this article. First, a nondimensional parameter  $K$  is introduced to distinguish the multiple steady state and oscillatory spatiotemporal patterns. These patterns play an important role in the understanding the mechanism of thermohaline circulation in different oceanic basins. Second, for both the multiple equilibria and periodic solutions transitions, both Type-I (continuous) and Type-II (jump) transitions can occur, depending respectively on the signs of two computable nondimensional parameters  $b_1$  and  $b_2$ .

A convection scale law is introduced, providing a method to introduce proper friction terms in the model in order to derive the correct circulation length scale. The analysis of the model with the proper friction terms shows that the THC appears to be associated with the continuous transitions to stable multiple equilibria.

The study provides some general principles and methods for the dynamic transitions and stability associated with thermohaline circulations, and will be used in different flow regimes in forthcoming articles.

## APPENDIX A. DYNAMIC TRANSITION THEORY FOR NONLINEAR SYSTEMS

In this appendix we recall some basic elements of the dynamic transition theory developed by the authors [17, 20], which are used to carry out the dynamic transition analysis in this article.

In sciences, nonlinear dissipative systems are generally governed by partial differential equations, which can be put in the perspective of a dynamical system, finite or infinite dimensional, as follows:

$$(A.1) \quad \frac{du}{dt} = L_\lambda u + G(u, \lambda), \quad u(0) = u_0,$$

where  $u : [0, \infty) \rightarrow H$  is the unknown function,  $\lambda \in \mathbb{R}^1$  is the system parameter, and  $H$  is a Banach space. We also need a Hilbert space  $H_1$  such that the inclusion  $H_1 \subset H$  is compact and dense.

**Linear theory and principle of exchange of stability.** Linear theory for system (A.1) is closely related to the principle of exchange of stability (PES), leading to precise information on linear unstable modes. To be precise, let  $\{\beta_j(\lambda) \in \mathbb{C} \mid j \in \mathbb{N}\}$  be the eigenvalues (counting multiplicity) of  $L_\lambda$ , and assume that

$$(A.2) \quad \operatorname{Re} \beta_i(\lambda) \begin{cases} < 0 & \text{if } \lambda < \lambda_0, \\ = 0 & \text{if } \lambda = \lambda_0, \\ > 0 & \text{if } \lambda > \lambda_0, \end{cases} \quad \forall 1 \leq i \leq m,$$

$$(A.3) \quad \operatorname{Re} \beta_j(\lambda_0) < 0 \quad \forall j \geq m + 1.$$

Much of the linear theory on stability and transitions is on establishing the PES. There are a vast literature devoted to linear theory including, among many others, [1, 8] for classical fluid dynamics, and [26] for geophysical fluid dynamics. Some formulas on the derivatives of the eigenvalues with respect to the control parameter are derived in [22], and are used to verify the PES in a much easier fashion.

**Center manifold reduction.** In many nonlinear problems, we need to reduce the infinite (or higher) dimensional system to a finite (or lower) dimensional system. The most natural way for this purpose is to project the underlying system

to the space generated by the most unstable modes, fully preserving the dynamic transition properties. This is achieved by using the center manifold reduction.

To be precise, assume that  $L_\lambda : H_1 \rightarrow H$  is a parameterized linear completely continuous field depending continuously on  $\lambda \in \mathbb{R}^1$ , which satisfies

$$(A.4) \quad \begin{aligned} L_\lambda &= -A + B_\lambda && \text{a sectorial operator,} \\ A &: H_1 \rightarrow H && \text{a linear homeomorphism,} \\ B_\lambda &: H_1 \rightarrow H && \text{a linear compact operator.} \end{aligned}$$

In this case, we can define the fractional order spaces  $H_\sigma$  for  $\sigma \in \mathbb{R}^1$ . Then we also assume that  $G(\cdot, \lambda) : H_\alpha \rightarrow H$  is  $C^r$  ( $r \geq 1$ ) bounded mapping for some  $0 \leq \alpha < 1$ , depending continuously on  $\lambda \in \mathbb{R}^1$ , and

$$(A.5) \quad G(u, \lambda) = o(\|u\|_{H_\alpha}) \quad \forall \lambda \in \mathbb{R}^1.$$

Hereafter we always assume the conditions (A.4) and (A.5), which represent that the system (A.1) has a dissipative structure. Then the type of transitions for (A.1) at  $(0, \lambda_0)$  is dictated by its reduction equation near  $\lambda = \lambda_0$  on the center manifold corresponding to the first  $m$  eigenvalues as given in (A.2) and (A.3):

$$(A.6) \quad \frac{dx}{dt} = J_\lambda x + g(x, \lambda) \quad \text{for } x \in \mathbb{R}^m,$$

where  $g(x, \lambda) = (g_1(x, \lambda), \dots, g_m(x, \lambda))$ , and

$$(A.7) \quad g_j(x, \lambda) = \langle G(\sum_{i=1}^m x_i e_i + \Phi(x, \lambda), \lambda), e_j^* \rangle \quad \forall 1 \leq j \leq m.$$

Here  $e_j$  and  $e_j^*$  ( $1 \leq j \leq m$ ) are the eigenvectors of  $L_\lambda$  and  $L_\lambda^*$  respectively corresponding to the eigenvalues  $\beta_j(\lambda)$  as in (A.2) and (A.3),  $J_\lambda$  is the  $m \times m$  order Jordan matrix corresponding to the first  $m$  eigenvalues, and  $\Phi(x, \lambda)$  is the center manifold function of (A.1) near  $\lambda_0$ . In addition, let

$$\begin{aligned} H &= E_1 \oplus E_2, \\ E_1 &= \text{span}\{e_i \mid 1 \leq i \leq m\}, \quad E_2 = E_1^\perp, \\ \mathcal{L}_\lambda &= L_\lambda|_{E_2}. \end{aligned}$$

The center manifold function  $\Phi$  is implicitly defined, and is oftentimes hard to compute. A systematic approach is developed in [15, 17, 20] to derive approximations of  $\Phi$ , which provide complete information on the dynamic transition of (A.6), consequently the original system (A.1). Suppose the nonlinear operator  $G$  to be of the form

$$(A.8) \quad G(u, \lambda) = G_k(u, \lambda) + o(\|u\|^k), \quad \text{as } u \rightarrow 0 \text{ in } H_\mu.$$

for some integer  $k \geq 2$ , where  $G_k$  is a  $k$ -multilinear operator

$$G_k(u, \lambda) = G_k(u, \dots, u, \lambda) : H_1 \times \dots \times H_1 \longrightarrow H.$$

**Theorem A.1.** [15] *Under the conditions (A.2), (A.3) and (A.8), the center manifold function  $\Phi(x, \lambda)$  can be expressed as*

$$(A.9) \quad \Phi(x, \lambda) = \int_{-\infty}^0 e^{-\tau \mathcal{L}_\lambda} \rho_\varepsilon P_2 G_k(e^{\tau J_\lambda} x, \lambda) d\tau + o(\|x\|^k),$$

where  $x = \sum_{i=1}^m x_i e_i \in E_1$ . In particular, we have the following assertions:

- (1) If  $J_\lambda$  is diagonal near  $\lambda = \lambda_0$ , then (A.9) can be written as
- (A.10) 
$$-\mathcal{L}_\lambda \Phi(x, \lambda) = P_2 G_k(x, \lambda) + o(\|x\|^k) + O(|\beta| \|x\|^k),$$
where  $\beta(\lambda) = (\beta_1(\lambda), \dots, \beta_m(\lambda))$  are the eigenvalues of  $J_\lambda$ .
- (2) Let  $m = 2$  and  $\beta_2(\lambda) = \overline{\beta_2(\lambda)} = \alpha(\lambda) + i\rho(\lambda)$  with  $\rho(\lambda_0) \neq 0$ . If  $G_k(u, \lambda) = G_2(u, \lambda)$  is bilinear, then the center manifold function  $\Phi(x, \lambda)$  can be expressed as

(A.11) 
$$\begin{aligned} & ((-\mathcal{L}_\lambda)^2 + 4\rho^2(\lambda))(-\mathcal{L}_\lambda)\Phi(x, \lambda) \\ &= ((-\mathcal{L}_\lambda)^2 + 4\rho^2(\lambda))P_2 G_2(x, \lambda) - 2\rho^2(\lambda)P_2 G_2(x, \lambda) \\ &+ 2\rho^2 P_2 G_2(x_1 e_2 - x_2 e_1) + \rho(-\mathcal{L}_\lambda)[G_2(x_1 e_1 + x_2 e_2, x_2 e_1 - x_1 e_2) \\ &+ G_2(x_2 e_1 - x_1 e_2, x_1 e_1 + x_2 e_2) + o(\|x\|^2) + O(|\alpha| \|x\|^2)]. \end{aligned}$$

**Classification of dynamic phase transitions.** A starting point of the dynamic transition theory is the introduction of a dynamic classification scheme of dynamic transitions, with which phase transitions, both equilibrium and non-equilibrium, are classified into three types: Type-I, Type-II and Type-III. Mathematically, Type-I, II and III transitions are also respectively called continuous, jump and mixed transitions. As we know, for equilibrium phase transitions, the usual classification scheme of phase transitions is based on the classical Ehrenfest classification scheme such that phase transitions are labeled by the lowest derivative of the free energy that is discontinuous at the transition.

Here we give a brief description about this classification. A state of the system (A.1) at  $\lambda$  is usually referred to a compact invariant set  $\Sigma_\lambda$ . A state  $\Sigma_\lambda$  of (A.1) is stable if  $\Sigma_\lambda$  is an attractor; otherwise  $\Sigma_\lambda$  is called unstable.

The system (A.1) undergoes a dynamic phase transition from a state  $\Sigma_\lambda$  at  $\lambda = \lambda_0$  if  $\Sigma_\lambda$  is stable on  $\lambda < \lambda_0$  and is unstable on  $\lambda > \lambda_0$ . The critical parameter  $\lambda_0$  is called a critical point. In other words, the phase transition corresponds to an exchange of stable states.

Assume that we have the linear theory at our disposal, i.e., the conditions (A.2) and (A.3) hold true. Then we can show that the system (A.1) undergoes a dynamic transition from  $(u, \lambda) = (0, \lambda_0)$ , and there is a neighborhood  $U \subset X$  of  $u = 0$  such that the transition is one of the three types, Type-I, II, and III as shown in Figures A.1-A.3; we refer interested readers to [15, 20]: Type-I (continuous)

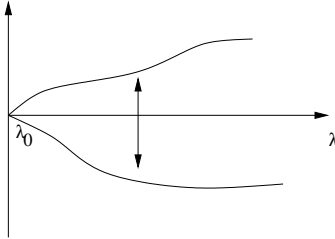


FIGURE A.1. Schematic of Type-I transition: The transition states are represented by a local attractor  $\Sigma_\lambda$ , which attracts a neighborhood of the basic solution.

transition is essentially determined by the attractor bifurcation theorem proved in

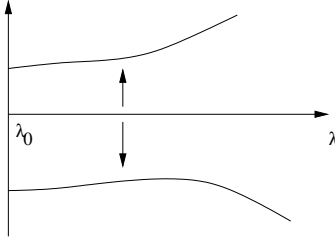


FIGURE A.2. Schematic of Type-II transition: The transition states are represented by some local attractors which are away from the basic state at the critical  $\lambda_0$ .

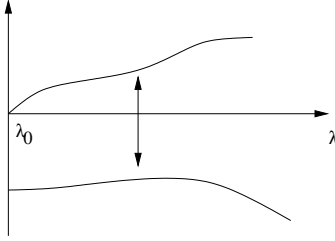


FIGURE A.3. Schematic of Type-III transition: The transition states are represented by two local attractors, with one as in a Type-II transition, and the other as in a Type-I transition.

[18, 17]. The attractor bifurcation theorem amounts to saying that when the PES holds true and the basic state is asymptotically stable at the critical parameter value  $\lambda_0$ , the system undergoes a Type-I dynamic transition, which is described by the bifurcated attractor. The study of the attractor bifurcation theory was initiated a few years ago by the authors, and has been applied to many problems in sciences. The key assumption here is the asymptotic stability of the basic solution at the critical parameter value  $\lambda_0$ . Two methods have been used to verify this condition in applications. One is a general alternative principle used in the study of Bénard convection [16, 17]. The other method is to use the center manifold reduction.

When the asymptotic stability of the basic state at the critical parameter is no longer valid, the system undergoes either Type-II or III transitions, depending on the nonlinear terms. Hereafter we list a few theorems, which are used directly in proving the main results in this article.

**Transitions from simple eigenvalues.** We consider the transition of (A.1) from a simple critical eigenvalue. Let the eigenvalues  $\beta_j(\lambda)$  of  $L_\lambda$  satisfy (A.2) and (A.3) with  $m = 1$ . Then the first eigenvalue  $\beta_1(\lambda)$  must be a real eigenvalue. Let  $e_1(\lambda)$  and  $e_1^*(\lambda)$  be the eigenvectors of  $L_\lambda$  and  $L_\lambda^*$  respectively corresponding to  $\beta_1(\lambda)$  with

$$L_{\lambda_0} e_1 = 0, \quad L_{\lambda_0}^* e_1^* = 0, \quad \langle e_1, e_1^* \rangle = 1.$$

Let  $\Phi(x, \lambda)$  be the center manifold function of (A.1) near  $\lambda = \lambda_0$ . We assume that

$$(A.12) \quad \langle G(xe_1 + \Phi(x, \lambda_0), \lambda_0), e_1^* \rangle = \alpha x^k + o(|x|^k),$$

where  $k \geq 2$  an integer and  $\alpha \neq 0$  a real number.

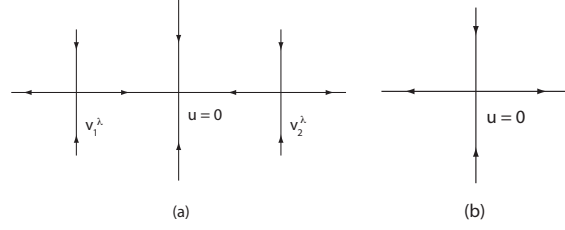


FIGURE A.4. Topological structure of the jump transition of (A.1) when  $k=\text{odd}$  and  $\alpha > 0$ : (a)  $\lambda < \lambda_0$ ; (b)  $\lambda \geq \lambda_0$ . Here the horizontal line represents the center manifold.

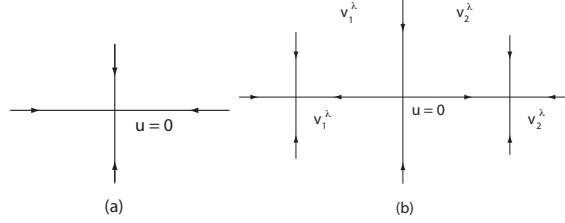


FIGURE A.5. Topological structure of the continuous transition of (A.1) when  $k=\text{odd}$  and  $\alpha < 0$ : (a)  $\lambda \leq \lambda_0$ ; (b)  $\lambda > \lambda_0$ .

**Theorem A.2.** *Assume (A.2) and (A.3) with  $m = 1$ , and (A.12). If  $k=\text{odd}$  and  $\alpha \neq 0$  in (A.12) then the following assertions hold true:*

- (1) *If  $\alpha > 0$ , then (A.1) has a jump transition from  $(0, \lambda_0)$ , and bifurcates on  $\lambda < \lambda_0$  to exactly two saddle points  $v_1^\lambda$  and  $v_2^\lambda$  with the Morse index one, as shown in Figure A.4.*
- (2) *If  $\alpha < 0$ , then (A.1) has a continuous transition from  $(0, \lambda_0)$ , which is an attractor bifurcation as shown in Figure A.5.*
- (3) *The bifurcated singular points  $v_1^\lambda$  and  $v_2^\lambda$  in the above cases can be expressed in the following form*

$$v_{1,2}^\lambda = \pm |\beta_1(\lambda)/\alpha|^{1/(k-1)} e_1(\lambda) + o(|\beta_1|^{1/(k-1)}).$$

When  $k=\text{even}$  and  $\alpha \neq 0$ , one can prove that there will be a mixed transition, we refer the interested readers to [20] for more details.

**Complex simple eigenvalues.** We now study the transition from a pair of complex eigenvalues. Assume that the eigenvalues of  $L_\lambda$  satisfy

$$(A.13) \quad \begin{cases} \text{Re}\beta_1(\lambda) = \text{Re}\beta_2(\lambda) \\ \text{Im}\beta_1(\lambda_0) = -\text{Im}\beta_2(\lambda_0) \neq 0, \end{cases} \begin{cases} < 0 & \text{if } \lambda < \lambda_0, \\ = 0 & \text{if } \lambda = \lambda_0, \\ > 0 & \text{if } \lambda > \lambda_0, \end{cases}$$

$$(A.14) \quad \text{Re}\beta_j(\lambda_0) < 0 \quad \forall j \geq 3.$$

It is known that with the conditions (A.13) and (A.14), (A.1) undergoes a Hopf bifurcation from  $(0, \lambda_0)$ . The following theorem amounts to saying that the transition of (A.1) from  $(0, \lambda_0)$  has only two types: continuous and jump transitions, which can be determined by the sign of a number  $b$  defined by (A.18).

For this purpose, let  $e_1(\lambda), e_2(\lambda)$  and  $e_1^*(\lambda)$  and  $e_2^*(\lambda)$  be the eigenvectors of  $L_\lambda$  and  $L_\lambda^*$  respectively corresponding to the complex eigenvalues  $\beta_2(\lambda) = \bar{\beta}_1(\lambda) = \alpha(\lambda) + i\delta(\lambda)$ , where  $\alpha$  satisfies (A.13),  $\sigma_0 = \sigma(\lambda_0) \neq 0$ , and

$$(A.15) \quad \begin{cases} L_\lambda e_1(\lambda) = \alpha(\lambda)e_1(\lambda) + \sigma(\lambda)e_2(\lambda), \\ L_\lambda e_2(\lambda) = -\sigma(\lambda)e_1(\lambda) + \alpha(\lambda)e_2(\lambda), \end{cases}$$

$$(A.16) \quad \begin{cases} L_\lambda^* e_1^*(\lambda) = \alpha(\lambda)e_1^* - \sigma(\lambda)e_2^*, \\ L_\lambda^* e_2^*(\lambda) = \sigma(\lambda)e_1^* + \alpha(\lambda)e_2^*. \end{cases}$$

By the spectral theorem in [17], we can take

$$\langle e_i(\lambda), e_j^*(\lambda) \rangle = \delta_{ij} \quad \forall 1 \leq i, j \leq 2.$$

Let  $\Phi(x, \lambda)$  be the center manifold function of (A.1) near  $\lambda = \lambda_0$ ,  $x = x_1 e_1 + x_2 e_2$ , and  $e_i = e_i(\lambda_0)$  ( $i = 1, 2$ ). Assume that for  $i = 1, 2$ ,

$$(A.17) \quad \langle G(x + \Phi(x, \lambda_0), \lambda_0), e_i^* \rangle = \sum_{2 \leq p+q \leq 3} a_{pq}^i x_1^p x_2^q + o(|x|^3).$$

For (A.17) we introduce a number, which is the bifurcation number:

$$(A.18) \quad b = \frac{3\pi}{4}(a_{30}^1 + a_{03}^2) + \frac{\pi}{4}(a_{12}^1 + a_{21}^2) + \frac{\pi}{2\sigma}(a_{02}^1 a_{02}^2 - a_{20}^1 a_{20}^2) \\ + \frac{\pi}{4\sigma}(a_{11}^1 a_{20}^1 + a_{11}^1 a_{02}^1 - a_{11}^2 a_{20}^2 - a_{11}^2 a_{02}^2).$$

Here

$$\sigma = \sigma(\lambda_0).$$

**Theorem A.3.** *Let the conditions (A.13) and (A.14) hold true.*

- (1) *If  $b < 0$ , then the transition of (A.1) is continuous, and the bifurcated periodic orbit is an attractor.*
- (2) *If  $b > 0$ , then the transition is jump, and (A.1) bifurcates on  $\lambda < \lambda_0$  to a unique unstable periodic orbit.*

**Singular separation.** We now study an important problem associated with the discontinuous transition of (A.1), which we call the singular separation.

**Definition A.1.** (1) *An invariant set  $\Sigma$  of (A.1) is called a singular element if  $\Sigma$  is either a singular point or a periodic orbit.*

- (2) *Let  $\Sigma_1 \subset X$  be a singular element of (A.1) and  $U \subset X$  a neighborhood of  $\Sigma_1$ . We say that (A.1) has a singular separation of  $\Sigma$  at  $\lambda = \lambda_1$  if*
  - (a) *(A.1) has no singular elements in  $U$  as  $\lambda < \lambda_1$  (or  $\lambda > \lambda_1$ ), and generates a singular element  $\Sigma_1 \subset U$  at  $\lambda = \lambda_1$ , and*
  - (b) *there are branches of singular elements  $\Sigma_\lambda$ , which are separated from  $\Sigma_1$  for  $\lambda > \lambda_1$  (or  $\lambda < \lambda_1$ ), i.e.,*

$$\lim_{\lambda \rightarrow \lambda_1} \max_{x \in \Sigma_\lambda} \text{dist}(x, \Sigma_1) = 0.$$

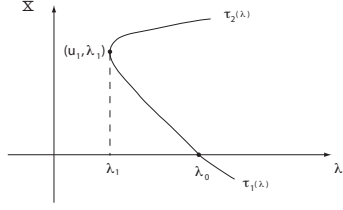


FIGURE A.6. Saddle-node bifurcation.

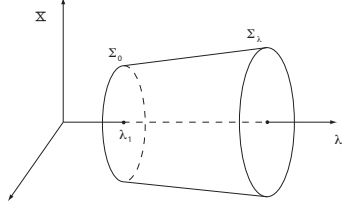


FIGURE A.7. Singular separation of periodic orbits.

A special case of singular separation is the saddle-node bifurcation. Intuitively, a saddle-node bifurcation is schematically shown as in Figure A.6, where the singular points in  $\Gamma_1(\lambda)$  are saddle points and in  $\Gamma_2(\lambda)$  are nodes, and the singular separation of periodic orbits is as in shown Figure A.7.

The following theorem gives a general principle for singular separation.

**Theorem A.4.** *Assume (A.2) and (A.3). Then the following assertions hold true:*

- (1) *If (A.1) bifurcates from  $(u, \lambda) = (0, \lambda_0)$  a branch  $\Sigma_\lambda$  of singular elements on  $\lambda < \lambda_0$  which is bounded in  $X \times (-\infty, \lambda_0)$  then (A.1) has a singular separation of singular elements at some  $(\Sigma_0, \lambda_1) \subset X \times (-\infty, \lambda_0)$ .*
- (2) *If the bifurcated branch  $\Sigma_\lambda$  consists of singular points which has index  $-1$ , i.e.,*

$$\text{ind}(-(L_\lambda + G), u_\lambda) = -1 \quad \forall u_\lambda \in E_\lambda, \quad \lambda < \lambda_0,$$

*then the singular separation is a saddle-node bifurcation from some  $(u_1, \lambda_1) \in X \times (-\infty, \lambda_0)$ .*

Consider the case where  $\beta_1(\lambda) = \beta_2(\lambda)$  are a pair of complex eigenvalues of  $L_\lambda$ , and assume that

$$(A.19) \quad \begin{aligned} \langle G(u, \lambda), u \rangle_H &= 0 & \forall u \in H_1, \\ \langle L_{\lambda^*} u, u \rangle_H &\leq -\alpha \|u\|_{H_{1/2}}^2 & \text{for some } \lambda^* < \lambda_0, \end{aligned}$$

or

$$(A.20) \quad \begin{aligned} \langle G(u, \lambda), u \rangle_H &\leq -c_1 \|u\|_H^p + c_2 \|u\|_H^2, \\ \langle L_\lambda u, u \rangle_H &\leq -\alpha \|u\|_{H_{1/2}}^2 + c_\lambda \|u\|_H^2, \end{aligned}$$

where  $\alpha, c_1, c_2 > 0$  are constants,  $p > 2$ ,  $c_\lambda \leq -c_2$  for some  $\lambda^* < \lambda_0$ , and  $\lambda_0$  is as in the PES (A.13) and (A.14).

**Theorem A.5.** *Under the PES (A.13) and (A.14), the equation (A.1) has the Hopf bifurcation at  $(0, \lambda_0)$ . If the branch  $\Sigma_\lambda$  of bifurcated periodic orbits is on  $\lambda < \lambda_0$ , then we have the following assertions:*

- (1) *If (A.19) holds, and for any  $\lambda$ , (A.1) possesses a global attractor in  $H$ , then (A.1) has a singular separation of periodic orbits at some  $(\Sigma_1, \lambda_1) \subset H \times (\lambda^*, \lambda_0)$ .*

- (2) If (A.20) holds true, then (A.1) has a singular separation of periodic orbits at some  $(\Sigma_1, \lambda_1) \subset H \times (\lambda^*, \lambda_0)$ .
- (3) The branch  $\Sigma_\lambda$  of bifurcated periodic orbits converges to  $\Sigma_1$  as  $\lambda \rightarrow \lambda_1$ .

### APPENDIX B. PROOF OF THE MAIN THEOREMS

**B.1. Proof of Theorem 3.1.** The proof of Theorem 3.1 is achieved using the following two lemmas.

The first lemma ensures that the R-Rayleigh number  $\sigma$  defined by (3.15) is a reasonable parameter describing the critical-crossing for the real eigenvalues of (3.1).

**Lemma B.1.** *Assume that*

$$\tilde{R} \neq \frac{-\text{Le}^2(1 + \text{Pr})\gamma_{j_1 k_1 1}^6}{(1 - \text{Le})\text{Pr}\alpha_{j_1 k_1}^2},$$

and for the R-Rayleigh number  $\sigma$  near  $\sigma_c$ , all real eigenvalues of (3.1) are given by

$$(B.1) \quad \beta_1 \geq \beta_2 \geq \dots \geq \beta_m \geq \beta_{m+1} \geq \dots.$$

Then  $\beta_1 = \beta_{j_1 k_1 1}^1$ , and

$$(B.2) \quad \beta_{j_1 k_1 1}(\sigma) \begin{cases} < 0 & \text{if } \sigma < \sigma_c, \\ = 0 & \text{if } \sigma = \sigma_c, \\ > 0 & \text{if } \sigma > \sigma_c, \end{cases}$$

where  $\sigma_c$  is as in (1.2).

*Proof.* Let  $\alpha = \alpha_{j_1 k_1}$ ,  $\gamma = \gamma_{j_1 k_1 1}$ ,  $R_0 - \text{Le}^{-1}\tilde{R}_0 = \gamma^6/\alpha^2$ , where  $(j_1, k_1)$  as in (1.2). We shall show that

$$(B.3) \quad (\text{Pr} + \text{Le} + \text{Pr Le})\gamma^4 - \text{Pr}\alpha^2\gamma^{-2}(R_0 - \tilde{R}_0) > 0.$$

Assume that (B.3) is not true, we consider the case

$$(B.4) \quad (\text{Pr} + \text{Le} + \text{Pr Le})\gamma^4 - \text{Pr}\alpha^2\gamma^{-2}(R_0 - \tilde{R}_0) < 0.$$

Note that the solution  $\beta(\sigma) = \beta_{j_1 k_1 1}^1(\sigma)$  of (3.14) with  $(j, k, l) = (j_1, k_1, 1)$  is continuous on  $\sigma$ , and  $\beta(\sigma_c) = 0$ . Hence

$$(B.5) \quad \beta(\sigma) \rightarrow 0 \quad \text{as } \sigma \rightarrow \sigma_c = R_0 - \text{Le}^{-1}\tilde{R}_0.$$

Thus, near  $\sigma = \sigma_c$  the equation (3.14) can be written as

$$(B.6) \quad \beta(\sigma) = \frac{-b_0(\sigma)}{b_1(\sigma)} + o(\beta(\sigma)),$$

where

$$(B.7) \quad \begin{aligned} b_0(\sigma) &= \text{Pr Le}\alpha^2 \left( \frac{\gamma^6}{\alpha^2} - \sigma \right), \\ b_1(\sigma) &= (\text{Pr} + \text{Le} + \text{Pr Le})\gamma^4 - \text{Pr}\alpha^2\gamma^2(R - \tilde{R}). \end{aligned}$$

It follows from (B.4)-(B.6) that

$$(B.8) \quad \beta(\sigma) \begin{cases} > 0 & \text{if } \sigma < \sigma_c, \\ = 0 & \text{if } \sigma = \sigma_c, \\ > 0 & \text{if } \sigma > \sigma_c. \end{cases}$$



for  $\sigma = R - \text{Le}^{-1}\tilde{R}$  near  $\sigma_c = R_0 - \text{Le}^{-1}\tilde{R}_0$ .

We write the equation (3.14) in the following form

$$(B.9) \quad \beta^3 + b_2\beta^2 + b_1(\sigma)\beta + b_0(\sigma) = 0$$

where  $b_0(\sigma), b_1(\sigma)$  are as in (B.7), and

$$b_2 = (\text{Pr} + \text{Le} + 1)\gamma^2 > 0.$$

Meanwhile, it is easy to see that

$$b_0(\sigma) \rightarrow +\infty, b_1(\sigma) \rightarrow +\infty, \text{ as } \sigma \rightarrow -\infty.$$

It implies that when  $\sigma$  is sufficiently small, the real solutions of (B.9) must be negative. Thus, by (B.8) there exists a number  $\sigma_0 < \sigma_c$  such that the solution  $\beta(\sigma)$  of (B.9) vanishes at  $\sigma = \sigma_0$  which is a contradiction to that  $b_0(\sigma_0) \neq 0$ . Thus, we derive  $b_1(\sigma_c) \geq 0$ . By the assumption in the lemma,  $b_1(\sigma_c) \neq 0$ . Hence, (B.3) holds true, i.e.,  $b_1(\sigma_c) > 0$ . By (B.6), we can obtain (B.2).

In the following, we shall prove that  $\beta_{j_1 k_1 1}^1 = \beta_1$  as in (B.1). We only need to consider the real eigenvalues  $\beta$  satisfying (3.14). Let  $\beta_m = \beta_{jkl}(\sigma_c)$  be a solution of (3.14) at  $\sigma = \sigma_c$ . We consider the coefficients of (3.14) at  $\sigma = \sigma_c$ . Thanks to (1.2),

$$\begin{aligned} & (\text{Pr} + \text{Le} + 1)\gamma_{jkl}^2 > 0, \\ & \text{Pr Le } \gamma_{jkl}^6 - \text{Pr } \alpha_{jk}^2 (\text{Le } R_0 - \tilde{R}) = \text{Pr } \alpha_{jk}^2 \text{Le} \left[ \frac{\gamma_{jkl}^6}{\alpha_{jk}^2} - \sigma_c \right] \geq 0. \end{aligned}$$

Thanks to (B.3), we have

$$\frac{(\text{Pr} + \text{Le} + \text{Pr Le})\gamma^6}{\text{Pr } \alpha^2} > R_0 - \tilde{R}_0.$$

Thus, we obtain

$$\begin{aligned} & (\text{Pr} + \text{Le} + \text{Pr Le})\gamma_{jkl}^4 - \text{Pr } \alpha_{jk}^2 \gamma_{jkl}^{-2} (R_0 - \tilde{R}_0) \\ &= \text{Pr } \alpha_{jk}^2 \gamma_{jkl}^{-2} \left[ \frac{\text{Pr} + \text{Le} + \text{Pr Le}}{\text{Pr}} \frac{\gamma_{jkl}^6}{\alpha_{jk}^2} - (R_0 - \tilde{R}_0) \right] \\ &> \alpha_{jk}^2 \gamma_{jkl}^{-2} (\text{Pr} + \text{Le} + \text{Pr Le}) \left( \frac{\gamma_{jkl}^6}{\alpha_{jk}^2} - \frac{\gamma^6}{\alpha^2} \right) \\ &> 0 \quad (\text{by (1.2)}). \end{aligned}$$

Hence, the coefficients of (3.14) at  $\sigma = \sigma_c$  are nonnegative, and strictly positive provided that  $\gamma_{jkl}^6/\alpha_{jk}^2 \neq \sigma_c$ . It follows that

$$\beta_m = \beta_{jkl}(\sigma_c) < 0 \quad \forall \sigma_c \neq \gamma_{jkl}^6/\alpha_{jk}^2.$$

Thus, we derive that  $\beta_{j_1 k_1 1} = \beta_1$  for  $\sigma$  near  $\sigma_c$ . The proof is complete.  $\square$

The following lemma shows that the C-Rayleigh number  $\eta$  defined by (3.17) characterizes the critical-crossing at  $\eta_c$  for the complex eigenvalues of (3.1).

**Lemma B.2.** *Let  $(j_1, k_1)$  satisfy (3.19), and the condition (3.18) hold true for  $(j, k, l) = (j_1, k_1, 1)$ . Then the pair of complex eigenvalues  $\beta_{j_1 k_1 1}^1(\eta) = \bar{\beta}_{j_1 k_1 1}^2(\eta)$  are*

critical-crossing at  $\eta = \eta_c$ :

$$\operatorname{Re}\beta_{j_1 k_1 1}^1(\eta) \begin{cases} < 0 & \text{if } \eta < \eta_c, \\ = 0 & \text{if } \eta = \eta_c, \\ > 0 & \text{if } \eta > \eta_c. \end{cases}$$

*Proof.* Near  $\eta = \eta_c$  the solution  $\beta_{j_1 k_1 1}^1(\eta)$  of (B.9) takes the form

$$(B.10) \quad \begin{aligned} \beta_{j_1 k_1 1}^1(\eta) &= \lambda(\eta) + i\rho(\eta), \\ \lambda(\eta) &\rightarrow 0, \quad \rho(\eta) \rightarrow \rho_0 \quad \text{as } \eta \rightarrow \eta_c. \end{aligned}$$

Inserting (B.10) into (B.9) we get

$$(B.11) \quad \begin{aligned} (-3\rho^2 + b_1)\lambda + b_0 - b_2\rho^2 + o(\lambda) &= 0, \\ -\rho^3 + \rho b_1 + 2\rho b_2\lambda + o(\lambda) &= 0. \end{aligned}$$

Since  $\rho_0 \neq 0$ , we derive from (B.11) that

$$\lambda(\eta) + o(\lambda) = \frac{b_0 - b_2\rho^2}{3\rho^2 - b_1} = \frac{b_0 - b_1 b_2 - 2b_2^2\lambda}{2b_1 + 6b_2\lambda} + o(\lambda),$$

which yields

$$(B.12) \quad \left(1 + \frac{b_2^2}{b_1}\right)\lambda(\eta) + o(\lambda) = \frac{b_0 - b_1 b_2}{2b_1 + 6b_2\lambda}.$$

Note that

$$\rho_0^2 = b_1(\eta_c) > 0, \quad \lambda(\eta_c) = 0.$$

We derive from (B.12) that

$$(B.13) \quad \operatorname{Re}\beta_{j_1 k_1 1}^1(\eta) = \lambda(\eta) \begin{cases} < 0 & \text{if } b_0 < b_1 b_2, \\ = 0 & \text{if } b_0 = b_1 b_2, \\ > 0 & \text{if } b_0 > b_1 b_2, \end{cases}$$

for  $\eta$  near  $\eta_c$ . It is easy to check that

$$b_0 \begin{cases} < b_1 b_2 & \text{if } \eta < \eta_c, \\ = b_1 b_2 & \text{if } \eta = \eta_c, \\ > b_1 b_2 & \text{if } \eta > \eta_c. \end{cases}$$

Thus, the lemma follows from (B.13).  $\square$

*Proof of Theorem 3.1.* Let  $\sigma = R - \operatorname{Le}^{-1}\tilde{R}$  be at the critical state

$$(B.14) \quad R - \operatorname{Le}^{-1}\tilde{R} = \sigma_c = \gamma^6/\alpha^2.$$

Assume that

$$(B.15) \quad \eta = R - \frac{\operatorname{Pr} + \operatorname{Le}}{\operatorname{Pr} + 1}\tilde{R} > \eta_c = \frac{(\operatorname{Pr} + \operatorname{Le})(1 + \operatorname{Le})}{\operatorname{Pr}} \frac{\gamma^6}{\alpha^2}.$$

Then, we deduce from (B.14) and (B.15) that

$$\tilde{R} \begin{cases} > \frac{\operatorname{Le}^2(\operatorname{Pr} + 1)}{(1 - \operatorname{Le})\operatorname{Pr}} \frac{\gamma^6}{\alpha^2} & \text{if } \operatorname{Le} < 1, \\ < \frac{\operatorname{Le}^2(\operatorname{Pr} + 1)}{(1 - \operatorname{Le})\operatorname{Pr}} \frac{\gamma^6}{\alpha^2} & \text{if } \operatorname{Le} > 1, \end{cases}$$

which implies that  $K < 0$ .

In addition, let  $\eta = \eta_c$ , namely

$$(B.16) \quad R - \frac{\text{Pr} + \text{Le}}{\text{Pr} + 1} \tilde{R} = \frac{(\text{Pr} + \text{Le})(1 + \text{Le})}{\text{Pr}} \frac{\gamma^6}{\alpha^2}.$$

Then noticing that  $K < 0$ , we can infer from (B.16) that

$$(B.17) \quad \rho_0^2 = (\text{Pr} + \text{Le} + \text{Pr Le})\gamma^4 - \text{Pr} \alpha^2 \gamma^{-2} (R - \tilde{R}) > 0,$$

Thus, by (B.17) and Lemma B.2, the conditions (B.14) and (B.15) imply that  $\eta_c$  is the first critical Rayleigh number, and (3.22) and (3.23) hold true.

Likewise, let

$$(B.18) \quad \eta = R - \frac{\text{Pr} + \text{Le}}{\text{Pr} + 1} \tilde{R} < \frac{(\text{Pr} + \text{Le})(1 + \text{Le})}{\text{Pr}} \frac{\gamma^6}{\alpha^2}.$$

Then, it is clear that (B.14) and (B.18) imply that  $\sigma_c$  is the first critical Rayleigh number, and

$$\tilde{R} \begin{cases} < \frac{\text{Le}^2(\text{Pr} + 1)}{(1 - \text{Le})\text{Pr}} \frac{\gamma^6}{\alpha^2} & \text{if } \text{Le} < 1, \\ > \frac{\text{Le}^2(\text{Pr} + 1)}{(1 - \text{Le})\text{Pr}} \frac{\gamma^6}{\alpha^2} & \text{if } \text{Le} > 1, \end{cases}$$

which implies  $K > 0$ .

By Lemma B.1 the conclusions (3.20) and (3.21) are valid. Thus, the theorem is proved.  $\square$

**B.2. Proof of Theorems 4.1–4.3.** The proof of these two theorems is based on the dynamical transition theory briefly presented in the Appendix. The central gravity of the proof is to carry out the detailed calculation of the center manifold reduction of the original infinite dimensional dynamical system to a finite dimensional dynamical systems.

*Proof of Theorems 4.1 and 4.2.* Let  $J_1 = (j_1, k_1, 1)$ ,  $\psi_{J_1} = \psi_{j_1 k_1}^1$ . The reduced equation of (2.6)-(2.8) in  $H$  reads

$$(B.19) \quad \frac{dx}{dt} = \beta_{J_1}^1(\sigma)x + \frac{1}{(\psi_{J_1}, \psi_{J_1}^*)} (G(\psi, \psi), \psi_{J_1}^*),$$

where  $\psi \in H$  is written as

$$(B.20) \quad \psi = x\psi_{J_1} + \Phi,$$

$\Phi$  is the center manifold function, and

$$G(\psi_1, \psi_2) = -P((u_1 \cdot \nabla)u_2, (u_1 \cdot \nabla)T_2, (u_1 \cdot \nabla)S_2),$$

$$(G(\psi_1, \psi_2), \psi_3) = - \int_{\Omega} \left[ \sum_{i,j=1}^3 u_{1i} \frac{\partial u_{2j}}{\partial x_i} u_{3j} + \sum_{i,j=1}^3 \left( u_{1i} \frac{\partial T_2}{\partial x_i} T_3 + u_{1i} \frac{\partial S_2}{\partial x_i} S_3 \right) \right] dx,$$

for  $\psi_i = (u_i, T_i, S_i) \in H$  ( $i = 1, 2, 3$ ).

By Theorem A.1, the center manifold function  $\Phi$  satisfies that

$$-L_{\lambda}\Phi = x^2 P_2 G(\psi_{J_1}, \psi_{J_1}) + \text{high order terms}.$$

Hence it is routine to calculate that

$$(B.21) \quad \Phi = x^2 \left[ \frac{(G(\psi_{J_1}, \psi_{J_1}), \psi_{2J}^*)}{-\beta_{2J}(\psi_{2J}, \psi_{2J}^*)} \psi_{2J} + \frac{(G(\psi_{J_1}, \psi_{J_1}), \psi_{002}^{1*})}{-\beta_{002}^1(\psi_{002}^1, \psi_{002}^{1*})} \psi_{002}^1 \right. \\ \left. + \frac{(G(\psi_{J_1}, \psi_{J_1}), \psi_{002}^{2*})}{-\beta_{002}^2(\psi_{002}^2, \psi_{002}^{2*})} \psi_{002}^2 \right] + o(2),$$

where

$$-\beta_{2J} = 4\text{Pr } \alpha^2, \quad -\beta_{002}^1 = 4\pi^2, \quad -\beta_{002}^2 = 4\text{Le } \pi^2,$$

and

$$\begin{aligned} \psi_{2J} = \psi_{2J}^* &= (k_1 \alpha_2 \sin 2j_1 \alpha_1 \pi x_1 \cos 2k_1 \alpha_2 \pi x_2, \\ &\quad -j_1 \alpha_1 \cos 2j_1 \alpha_1 \pi x_1 \sin 2k_1 \alpha_2 \pi x_2, 0, 0, 0), \\ \psi_{002}^1 = \psi_{002}^{1*} &= (0, 0, 0, \sin 2\pi x_3, 0), \\ \psi_{002}^2 = \psi_{002}^{2*} &= (0, 0, 0, 0, \sin 2\pi x_3). \end{aligned}$$

Inserting (B.20) into (B.19), we have

$$(B.22) \quad \frac{dx}{dt} = \beta_{J_1}^1(\sigma)x - \delta(\sigma)x^3 + o(3),$$

where

$$\begin{aligned} \delta(\sigma_c) &= \sum_{(J,i) \neq (J_1,1)} \frac{(G(\psi_{J_1}, \psi_{J_1}), \psi_{J_i}^{i*}) [(G(\psi_{J_1}, \psi_{J_1}^*), \psi_{J_i}^i) + (G(\psi_{J_i}^i, \psi_{J_1}^*), \psi_{J_1})]}{-\beta_{J_i}^i(\psi_{J_1}, \psi_{J_1}^*)(\psi_{J_i}^i, \psi_{J_i}^{i*})} \\ &= \frac{1}{(\psi_{J_1}, \psi_{J_1}^*)} \left[ \frac{(G(\psi_{J_1}, \psi_{J_1}), \psi_{2J}^*)(G(\psi_{J_1}, \psi_{J_1}^*), \psi_{2J})}{-\beta_{2J}(\psi_{2J}, \psi_{2J}^*)} \right. \\ &\quad + \frac{(G(\psi_{J_1}, \psi_{J_1}), \psi_{002}^{1*})(G(\psi_{J_1}, \psi_{J_1}^*), \psi_{002}^1)}{-\beta_{002}^1(\psi_{002}^1, \psi_{002}^{1*})} \\ &\quad \left. + \frac{(G(\psi_{J_1}, \psi_{J_1}), \psi_{002}^{2*})(G(\psi_{J_1}, \psi_{J_1}^*), \psi_{002}^2)}{-\beta_{002}^2(\psi_{002}^2, \psi_{002}^{2*})} \right] \\ &= \frac{\pi^2}{8(\psi_{J_1}, \psi_{J_1}^*)} \left[ \frac{(k_1 \alpha_2 u_{J_1} - J_1 \alpha_1 v_{J_1})(k_1 \alpha_2 u_{J_1}^* - J_1 \alpha_1 v_{J_1}^*)}{\text{Pr } \alpha^4} + \frac{T_{J_1} T_{J_1}^*}{\pi^4} + \frac{S_{J_1} S_{J_1}^*}{\pi^4 \text{Le}} \right]. \end{aligned}$$

Here

$$\begin{aligned} u_{J_1} = u_{J_1}^* &= -\frac{j_1 \alpha_1 \pi^2}{\alpha^2}, & v_{J_1} = v_{J_1}^* &= -\frac{k_1 \alpha_2 \pi^2}{\alpha^2}, \\ T_{J_1} &= \frac{1}{\gamma^2 + \beta_{J_1}^1}, & T_{J_1}^* &= \frac{\text{Pr } R}{\gamma^2 + \beta_{J_1}^1}, \\ S_{J_1} &= \frac{\text{sign}(S_0 - S_1)}{\text{Le } \gamma^2 + \beta_{J_1}^1}, & S_{J_1}^* &= \frac{\text{Pr } \tilde{R} \text{ sign}(S_0 - S_1)}{\text{Le } \gamma^2 + \beta_{J_1}^1}. \end{aligned}$$

By  $\beta_{J_1}(\sigma_c) = 0$ , direct calculation yields that at  $\sigma = \sigma_c$ ,

$$\delta(\sigma_c) = \frac{\text{Pr}(\text{Le}^3 R - \tilde{R})}{8\pi^2 \gamma^4 \text{Le}^3(\psi_{J_1}, \psi_{J_1}^*)} = \frac{\text{Le}^3 R - \tilde{R}}{8\pi^2 \text{Le}^3 \left( \frac{\sigma_c}{\text{Pr}} + R - \frac{\tilde{R}}{\text{Le}^2} \right)}.$$

Putting  $R = \text{Le}^{-1} \tilde{R} + \sigma_c$  into  $\delta(\sigma_c)$ , we derive that

$$\delta = \delta(\sigma_c) = \frac{1}{8\pi^2 \text{Le}^3} \frac{\text{Le}^3 \sigma_c - (1 - \text{Le}^2) \tilde{R}}{\left(1 + \frac{1}{\text{Pr}}\right) \sigma_c - \frac{1 - \text{Le}}{\text{Le}^2} \tilde{R}}.$$

Hence using  $K > 0$ , the sign of  $\delta$  is the same as the sign of  $b_1$  defined by (1.3), and then the theorem follows from Theorems A.2 and A.4, and from (B.22).  $\square$

*Proof of Theorem 4.3.* Let  $J = (j_1, 0, 1)$  and  $\beta(\eta) = \beta_J^1(\eta) = \lambda(\eta) + i\rho(\eta)$  be the first eigenvalue of (B.10) near  $\eta = \eta_c$  with

$$(B.23) \quad \lambda(\eta_c) = 0, \quad \rho(\eta_c) = \rho > 0.$$

By (B.23), the eigenvectors  $\psi_J = \psi_J^1 + i\psi_J^2$  corresponding to  $\beta(\eta)$  are given by

$$\begin{aligned} \psi_J^1 &= \left( -\frac{1}{j_1\alpha_1} \sin \phi \cos \pi x_3, 0, \cos \phi \sin \pi x_3, \right. \\ &\quad \left. ReA_2(\beta) \cos \phi \sin \pi x_3, ReA_3(\beta) \cos \phi \sin \pi x_3 \right), \\ \psi_J^2 &= (0, 0, 0, ImA_2(\beta) \cos \phi \sin \pi x_3, ImA_3(\beta) \cos \phi \sin \pi x_3), \end{aligned}$$

where  $\phi = j_1\alpha_1\pi x_1$ . By (3.13) the conjugate eigenvectors  $\psi_J^* = \psi_J^{1*} + i\psi_J^{2*}$  are given by

$$\begin{aligned} \psi_J^{1*} &= \left( -\frac{1}{j_1\alpha_1} \sin \phi \cos \pi x_3, 0, \cos \phi_1 \sin \pi x_3, \right. \\ &\quad \left. Pr RReA_2(\bar{\beta}) \cos \phi \sin \pi x_3, -Pr \tilde{R}ReA_3(\bar{\beta}) \cos \phi \sin \pi x_3 \right), \\ \psi_J^{2*} &= (0, 0, 0, Pr RImA_2(\bar{\beta}) \cos \phi \sin \pi x_3, -Pr \tilde{R}ImA_3(\bar{\beta}) \cos \phi \sin \pi x_3) \end{aligned}$$

and

$$(B.24) \quad A_2(\beta) = \frac{1}{\alpha^2 + \pi^2 + \beta}, \quad A_3(\beta) = \frac{1}{Le(\alpha^2 + \pi^2) + \beta}.$$

The conjugate eigenvectors  $\Phi_J^{1*}$  and  $\Phi_J^{2*}$ , satisfying

$$(\psi_J^1, \Phi_J^{1*}) = (\psi_J^2, \Phi_J^{2*}) \neq 0, \quad (\psi_J^1, \Phi_J^{2*}) = (\psi_J^2, \Phi_J^{1*}) = 0,$$

are given by

$$(B.25) \quad \Phi_J^{1*} = \psi_J^{1*} + C\psi_J^{2*}, \quad \Phi_J^{2*} = -C\psi_J^{1*} + \psi_J^{2*},$$

where

$$(B.26) \quad C = \frac{(\psi_J^1, \psi_J^{2*})}{(\psi_J^1, \psi_J^{1*})} = -\frac{(\psi_J^2, \psi_J^{1*})}{(\psi_J^2, \psi_J^{2*})} = \frac{B_2}{B_1}.$$

The reduced equations of (2.6)-(2.8) read

$$(B.27) \quad \begin{aligned} \frac{dx}{dt} &= \lambda x + \rho y + \frac{1}{(\psi_J^1, \Phi_J^{1*})} (G(\psi, \psi), \Phi_J^{1*}), \\ \frac{dy}{dt} &= -\rho x + \lambda y + \frac{1}{(\psi_J^2, \Phi_J^{2*})} (G(\psi, \psi), \Phi_J^{2*}), \end{aligned}$$

where  $\psi \in H$  is as

$$(B.28) \quad \psi = x\psi_J^1 + y\psi_J^2 + \Phi,$$

and  $\Phi$  is the center manifold function.

Note that for any gradient field  $\nabla\varphi$ , the Leray projection  $P(\nabla\varphi) = 0$ . Therefore, by (B.25)-(B.26) we have

$$\begin{aligned} G(\psi_J^1, \psi_J^1) &= \frac{\pi}{2}(0, 0, 0, \operatorname{Re}A_2 \sin 2\pi x_3, \operatorname{Re}A_3 \sin 2\pi x_3), \\ G(\psi_J^1, \psi_J^2) &= \frac{\pi}{2}(0, 0, 0, \operatorname{Im}A_2 \sin 2\pi x_3, \operatorname{Im}A_3 \sin 2\pi x_3), \\ G(\psi_J^1, \Phi_J^{1*}) &= \frac{\pi \operatorname{Pr}}{2B_1}(0, 0, 0, R(B_1 \operatorname{Re}A_2 - B_2 \operatorname{Im}A_2) \sin 2\pi x_3, \\ &\quad - \tilde{R}(B_1 \operatorname{Re}A_3 - B_2 \operatorname{Im}A_3) \sin 2\pi x_3) \\ G(\psi_J^1, \Phi_J^{2*}) &= \frac{\pi \operatorname{Pr}}{2B_1}(0, 0, 0, -R(B_2 \operatorname{Re}A_2 + B_1 \operatorname{Im}A_2) \sin 2\pi x_3, \\ &\quad \tilde{R}(B_2 \operatorname{Re}A_3 + B_1 \operatorname{Im}A_3) \sin 2\pi x_3) \\ G(\psi_J^2, \psi) &= 0, \quad \forall \psi \in H. \end{aligned}$$

Hence, by (A.11), the center manifold function  $\Phi$  is expressed as

$$(B.29) \quad \Phi = \Phi_1 + \Phi_2 + \Phi_3 + o(2),$$

where  $G_{ij} = G(\psi_J^i, \psi_J^j)$ , and

$$\begin{aligned} \Phi_1 &= -\frac{\psi_{002}^1}{\beta_{002}^1 \|\psi_{002}^1\|^2} [x^2(G_{11}, \psi_{002}^1) + xy(G_{12}, \psi_{002}^1)] \\ &\quad - \frac{\psi_{002}^2}{\beta_{002}^2 \|\psi_{002}^2\|^2} [x^2(G_{11}, \psi_{002}^2) + xy(G_{12}, \psi_{002}^2)], \\ \Phi_2 &= \frac{2\rho^2 \psi_{002}^1}{\beta_{002}^1 (\beta_{002}^{12} + 4\rho^2) \|\psi_{002}^1\|^2} [(x^2 - y^2)(G_{11}, \psi_{002}^1) + 2xy(G_{12}, \psi_{002}^1)] \\ &\quad + \frac{2\rho^2 \psi_{002}^2}{\beta_{002}^2 ((\beta_{002}^2)^2 + 4\rho^2) \|\psi_{002}^2\|^2} [(x^2 - y^2)(G_{11}, \psi_{002}^2) + 2xy(G_{12}, \psi_{002}^2)], \\ \Phi_3 &= \frac{\rho \psi_{002}^1}{((\beta_{002}^1)^2 + 4\rho^2) \|\psi_{002}^1\|^2} [2xy(G_{11}, \psi_{002}^1) + (y^2 - x^2)(G_{12}, \psi_{002}^1)] \\ &\quad + \frac{\rho \psi_{002}^2}{((\beta_{002}^2)^2 + 4\rho^2) \|\psi_{002}^2\|^2} [2xy(G_{11}, \psi_{002}^2) + (y^2 - x^2)(G_{11}, \psi_{002}^2)]. \end{aligned}$$

It is clear that

$$(G(\Phi, \Phi_J^{i*}), \psi_J^j) = o(2) \quad \forall i, j = 1, 2.$$

Then, inserting (B.28) into (B.27), one gets

$$(B.30) \quad \begin{aligned} \frac{dx}{dt} &= \lambda x + \rho y - \frac{x(G(\psi_J^1, \Phi_J^{1*}), \Phi)}{(\psi_J^1, \Phi_J^{1*})} + o(3), \\ \frac{dy}{dt} &= -\rho x + \lambda y - \frac{x(G(\psi_J^1, \Phi_J^{2*}), \Phi)}{(\psi_J^2, \Phi_J^{2*})} + o(3). \end{aligned}$$

From (B.29) and (B.30) it follows that

$$(B.31) \quad \begin{aligned} \frac{dx}{dt} &= \lambda x + \rho y + \frac{\operatorname{Pr} \pi x [a_1 x^2 + a_2 xy + a_3 y^2]}{(\psi_J^1, \psi_J^{1*})^2 + (\psi_J^1, \psi_J^{2*})^2} + o(3), \\ \frac{dy}{dt} &= -\rho x + \lambda y + \frac{\operatorname{Pr} \pi x [b_1 x^2 + b_2 xy + b_3 y^2]}{(\psi_J^1, \psi_J^{1*})^2 + (\psi_J^1, \psi_J^{2*})^2} + o(3), \end{aligned}$$

where

$$\begin{aligned} a_1 &= R(-R_2B_1 + I_2B_2)D_1 + \tilde{R}(R_3B_1 - I_3B_2)F_1 \\ a_3 &= R(-R_2B_1 + I_2B_2)D_3 + \tilde{R}(R_3B_1 - I_3B_2)F_3 \\ b_2 &= R(I_2B_1 + R_2B_2)D_2 - \tilde{R}(I_3B_1 + R_3B_2)F_2 \end{aligned}$$

where  $B_1, B_2$  are as in (B.26), and

$$\begin{aligned} D_1 &= \frac{R_2}{8\pi} - \frac{\rho^2 R_2}{16\pi(4\pi^4 + \rho^2)} + \frac{\rho\pi I_2}{4(4\pi^4 + \rho^2)}, \\ D_2 &= \frac{I_2}{8\pi} - \frac{\rho^2 I_2}{8\pi(4\pi^4 + \rho^2)} - \frac{\rho\pi R_2}{4(4\pi^4 + \rho^2)}, \\ D_3 &= \frac{\rho^2 R_2}{16\pi(4\pi^4 + \rho^2)} - \frac{\rho\pi I_2}{8(4\pi^4 + \rho^2)}, \\ F_1 &= \frac{R_3}{8\pi\text{Le}} - \frac{\rho^2 R_3}{16\pi\text{Le}(4\pi^4\text{Le}^2 + \rho^2)} - \frac{\rho I_3}{8(4\pi^4\text{Le}^2 + \rho^2)}, \\ F_2 &= \frac{I_3}{8\pi\text{Le}} - \frac{\rho^2 I_3}{8\pi\text{Le}(4\pi^4\text{Le}^2 + \rho^2)} + \frac{\rho R_3}{4(4\pi^4\text{Le}^2 + \rho^2)}, \\ F_3 &= \frac{\rho^2 R_3}{16\pi\text{Le}(4\pi^4\text{Le}^2 + \rho^2)} + \frac{\rho I_3}{8(4\pi^4\text{Le}^2 + \rho^2)}. \end{aligned}$$

Then we obtain

$$\begin{aligned} \text{(B.32)} \quad b &= 3a_1 + a_3 + b_2 \\ &= \frac{1}{4}[R(R_2B_1 - I_2B_2)C_3 + R(I_2B_1 + R_2B_2)C_4 \\ &\quad + \tilde{R}(R_3B_1 - I_3B_2)C_5 + \tilde{R}(I_3B_1 + R_3B_2)C_6] \\ &= \frac{1}{4}b_2, \end{aligned}$$

where  $b_2$  is the number defined by (4.2).

By (B.31)-(B.32), this theorem follows from Theorems A.3 and A.5. The proof is complete.  $\square$

#### REFERENCES

- [1] S. CHANDRASEKHAR, *Hydrodynamic and Hydromagnetic Stability*, Dover Publications, Inc., 1981.
- [2] H. A. DIJKSTRA, *Nonlinear Physical Oceanography: A Dynamical Systems Approach to the Large Scale Ocean Circulation and El Niño.*, Kluwer Academic Publishers, Dordrecht, the Netherlands, 2000.
- [3] H. A. DIJKSTRA AND M. GHIL, *Low-frequency variability of the large-scale ocean circulations: a dynamical systems approach*, *Review of Geophysics*, 43 (2005), pp. 1–38.
- [4] H. A. DIJKSTRA AND M. J. MOLEMAKER, *Symmetry breaking and overturning oscillations in thermohaline-driven flows*, *J. Fluid Mech.*, 331 (1997), p. 195232.
- [5] ———, *Imperfections of the north-atlantic wind-driven ocean circulation: Continental geometry and wind stress shape*, *J. Mar. Res.*, 57 (1999), pp. 1–28.
- [6] H. A. DIJKSTRA AND J. D. NEELIN, *Imperfections of the thermohaline circulation: Multiple equilibria and flux-correction*, *J. Clim.*, 12 (1999), p. 13821392.
- [7] ———, *Imperfections of the thermohaline circulation: Latitudinal asymmetry versus asymmetric freshwater flux*, *J. Clim.*, 13 (2000), pp. 366–382.
- [8] P. DRAZIN AND W. REID, *Hydrodynamic Stability*, Cambridge University Press, 1981.
- [9] M. GHIL, *Climate stability for a sellers-type model*, *J. Atmos. Sci.*, 33 (1976), p. 320.

- [10] M. GHIL AND S. CHILDRESS, *Topics in Geophysical Fluid Dynamics: Atmospheric Dynamics, Dynamo Theory, and Climate Dynamics*, Springer-Verlag, New York, 1987.
- [11] I. M. HELD AND M. J. SUAREZ, *Simple albedo feedback models of the ice caps*, *Tellus*, 26 (1974), p. 613629.
- [12] C.-H. HSIA, T. MA, AND S. WANG, *Attractor bifurcation of three dimensional double-diffusive convection*, *ZAA*, 27 (2008), pp. 233–252.
- [13] ———, *Bifurcation and stability of two-dimensional double-diffusive convection*, *Commun. Pure Appl. Anal.*, 7 (2008), pp. 23–48.
- [14] J.-L. LIONS, R. TEMAM, AND S. H. WANG, *On the equations of the large-scale ocean*, *Nonlinearity*, 5 (1992), pp. 1007–1053.
- [15] T. MA AND S. WANG, *Phase Transition Dynamics in Nonlinear Sciences*, in preparation.
- [16] ———, *Dynamic bifurcation and stability in the Rayleigh-Bénard convection*, *Commun. Math. Sci.*, 2 (2004), pp. 159–183.
- [17] ———, *Bifurcation theory and applications*, vol. 53 of World Scientific Series on Nonlinear Science. Series A: Monographs and Treatises, World Scientific Publishing Co. Pte. Ltd., Hackensack, NJ, 2005.
- [18] ———, *Dynamic bifurcation of nonlinear evolution equations*, *Chinese Ann. Math. Ser. B*, 26 (2005), pp. 185–206.
- [19] ———, *Rayleigh-Bénard convection: dynamics and structure in the physical space*, *Commun. Math. Sci.*, 5 (2007), pp. 553–574.
- [20] ———, *Stability and Bifurcation of Nonlinear Evolutions Equations*, Science Press, 2007.
- [21] ———, *Dynamic model and phase transitions for liquid helium*, *Journal of Mathematical Physics*, 49:073304 (2008), pp. 1–18.
- [22] ———, *Exchange of stabilities and dynamic transitions*, *Georgian Mathematics Journal*, 15:3 (2008), pp. 581–590.
- [23] ———, *Phase transition and separation for mixture of liquid he-3 and he-4, in a special issue dedicated to the legacy of landau*, *EJTP*, (2008).
- [24] ———, *Superfluidity of helium-3*, *Physica A: Statistical Mechanics and its Applications*, 387:24 (2008), pp. 6013–6031.
- [25] W. V. R. MALKUS AND G. VERONIS, *Finite amplitude cellular convection*, *J. Fluid Mech.*, 4 (1958), pp. 225–260.
- [26] J. PEDLOSKY, *Geophysical Fluid Dynamics*, Springer-Verlag, New-York, second ed., 1987.
- [27] C. QUON AND M. GHIL, *Multiple equilibria in thermosolutal convection due to salt-flux boundary conditions*, *J. Fluid Mech.*, 245 (1992), p. 449484.
- [28] ———, *Multiple equilibria and stable oscillations in thermosolutal convection at small aspect ratio*, *J. Fluid Mech.*, 291 (1995), pp. 33–56.
- [29] C. Rooth, *Hydrology and ocean circulation*, *Prog. Oceanogr.*, 11 (1982), p. 131149.
- [30] R. M. SAMELSON AND G. K. VALLIS, *Large-scale circulation with small diapycnal diffusion: the two-thermocline limit*, *Journal of Marine Research*, 55 (1997), pp. 223–275.
- [31] ———, *A simple friction and diffusion scheme for planetary geostrophic basin models*, *Journal of Physical Oceanography*, 27 (1997), pp. 186–194.
- [32] M. E. STERN, *The “salt fountain” and thermohaline convection*, *Tellus*, 12 (1960), pp. 172–175.
- [33] H. STOMMEL, *Thermohaline convection with two stable regimes of flow*, *Tellus*, 13 (1961), pp. 224–230.
- [34] O. THUAL AND J. C. MCWILLIAMS, *The catastrophe structure of thermohaline convection in a two-dimensional fluid model and a comparison with low-order box models*, *Geophys. Astrophys. Fluid Dyn.*, 64 (1992), p. 6795.
- [35] E. TZIPERMAN, *Inherently unstable climate behavior due to weak thermohaline ocean circulation*, *Nature*, 386 (1997), p. 592595.
- [36] E. TZIPERMAN, J. R. TOGGWEILER, Y. FELIKS, AND K. BRYAN, *Instability of the thermohaline circulation with respect to mixed boundary conditions: Is it really a problem for realistic models?*, *J. Phys. Oceanogr.*, 24 (1994), p. 217232.

(TM) DEPARTMENT OF MATHEMATICS, SICHUAN UNIVERSITY, CHENGDU, P. R. CHINA

(SW) DEPARTMENT OF MATHEMATICS, INDIANA UNIVERSITY, BLOOMINGTON, IN 47405  
*E-mail address:* showang@indiana.edu, <http://www.indiana.edu/~fluid>